Task-Level Approaches for the Control of Constrained Multibody Systems

Vincent De Sapio and Oussama Khatib
Artificial Intelligence Laboratory
Computer Science Department
Stanford University
Stanford, CA 94305, USA
{vdesap, khatib}@robotics.stanford.edu

Scott Delp
Neuromuscular Biomechanics Laboratory
Mechanical Engineering & Bioengineering Departments
Stanford University
Stanford, CA 94305, USA
delp@stanford.edu

April 26, 2006

Abstract

This paper presents a task-level control methodology for the general class of holonomically constrained multibody systems. As a point of departure, the general formulation of constrained dynamical systems is reviewed with respect to multiplier and minimization approaches. Subsequently, the operational space framework is considered and the underlying symmetry between constrained dynamics and operational space control is discussed. Motivated by this symmetry, approaches for constrained task-level control are presented which cast the general formulation of constrained multibody systems into a task space setting using the operational space framework. This provides a means of exploiting task-level control structures, native to operational space control, within the context of constrained systems. This allows us to naturally synthesize dynamic compensation for a multibody system, that properly accounts for the system constraints while performing a control task. A set of examples illustrate this control implementation. Additionally, the inclusion of flexible bodies in this approach is addressed.

Keywords: task-level control, constrained multibody dynamics, operational space, null space, flexible/rigid multibody system

1 Introduction

The control of multibody systems is of interest to a number of research communities in a variety of application areas. In particular, the robotics community has focussed on the control of high degree-of-freedom robotic systems. Typically, this has involved the control of serial and branching chain systems. The traditional approach for controlling these systems has been joint space (ie., configuration space) control. The operational space approach was introduced by Khatib [15] [16] to simplify the control problem by specifying a *task space* rather than a joint space control objective. Task space is used interchangeably with operational space to refer to the space of motion control coordinates. As one simple example, the task space for controlling a robot arm can be defined as the Cartesian space used to describe the position of the end effector. Using the operational space approach the configuration space dynamics of a multibody system are mapped into an appropriate task space. This is advantageous for control purposes since the operational space method provides task-level dynamic models and structures for decoupled task and posture control. This allows for posture objectives to be controlled without dynamically interfering with the primary task(s).

The benefits of operational space control have been primarily exploited for serial and branching chain systems. However, there has been substantially less emphasis on the use of operational space control for closed chain or parallel systems, like the structures of *Figure 1* [6]. Closed chains are a subset of the larger class of holonomically constrained systems which include biomechanical structures such as the knee and shoulder complex of *Figure 2*. Rather than loop closures these examples involve constraints internal to the branching chains [8] [11], expressed as algebraic dependencies between the generalized coordinates.

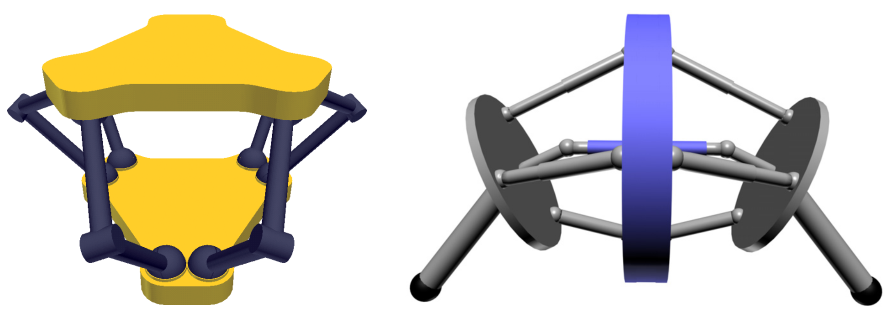

Figure 1: Parallel mechanisms consisting of serial chains with loop closures described by a set of holonomic constraints. (Left) A spatial positioning platform [6]. (Right) Bilateral representation of a parallel-serial robotic shoulder mechanism [19].

This paper addresses the use of task-level approaches for the control of holonomically constrained multibody systems. As a point of departure, the general formulation of constrained dynamical systems is reviewed. This entails an elaboration of multiplier and minimization forms of the constrained multibody equations of motion. The basis for task-level control is then presented with a review of the operational space method. Operational space dynamic consistency provides a mechanism for exploring the underlying symmetry between task and constraint dynamics.

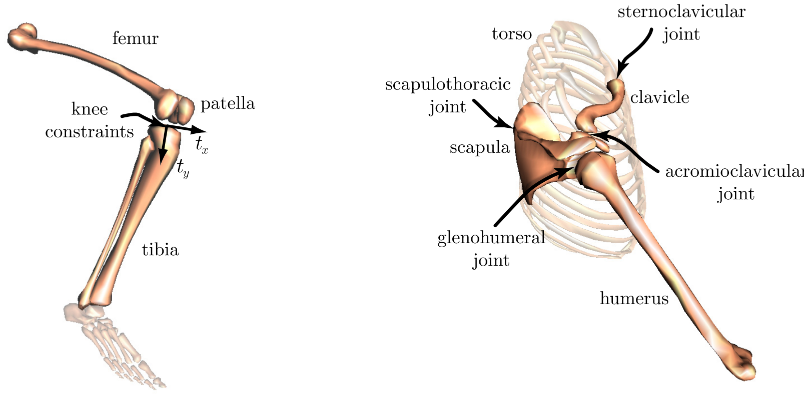

Figure 2: Holonomic constraints provide more physiologically representative models. (Left) The tibia translates as a function of knee flexion [8]. (Right) The shoulder girdle (scapula and clavicle) is kinematically coupled to the glenohumeral joint [11].

Formulations for constrained task-level control are then be presented, punctuated with a set of examples. Finally, the inclusion of flexible bodies in this approach is discussed.

2 Constrained Dynamics

The subsequent sections review the dynamical formulation of constrained multibody systems. This review covers the well known method of Lagrange multipliers, a multiplier elimination method, and the less well known minimization formalism of Gauss' Principle. This latter formalism naturally leads to an explicit solution of the constrained dynamical system and the subsequent formulation of a generalized constrained equation of motion. The multiplier form, the eliminated multiplier form, and the generalized constrained form will each be used in *Section 5* to formulate novel methods for constrained operational space control.

2.1 Unconstrained Systems

The equations of motion for a multibody system that is unconstrained with respect to configuration space are expressed in standard form as [3],

$$\boldsymbol{M}(\boldsymbol{q})\,\ddot{\boldsymbol{q}} + \boldsymbol{b}(\boldsymbol{q},\dot{\boldsymbol{q}}) = \boldsymbol{f}(\boldsymbol{q},\dot{\boldsymbol{q}}) + \boldsymbol{B}(\boldsymbol{q},\dot{\boldsymbol{q}})^T\boldsymbol{u} \tag{1}$$

where $\boldsymbol{q}$ is the $n \times 1$ vector of generalized coordinates, $\boldsymbol{u}$ is the $k \times 1$ vector of control inputs, $\boldsymbol{B}(\boldsymbol{q},\dot{\boldsymbol{q}})^T$ is the $n \times k$ matrix mapping control inputs to generalized actuator forces, $\boldsymbol{M}(\boldsymbol{q})$ is the $n \times n$ mass matrix, $\boldsymbol{b}(\boldsymbol{q},\dot{\boldsymbol{q}})$ is the $n \times 1$ vector of centrifugal and Coriolis terms, and $\boldsymbol{f}(\boldsymbol{q},\dot{\boldsymbol{q}})$ is the $n \times 1$ vector of generalized applied forces. For conciseness we will often refrain from explicitly denoting the functional dependence of these quantities on $\boldsymbol{q}$ and $\dot{\boldsymbol{q}}$. This practice will also be employed with other quantities as well.

Throughout this paper we will use a modified and more specialized form of (1) common in robotics [5],

$$\boldsymbol{\tau} = \boldsymbol{M}(\boldsymbol{q})\,\ddot{\boldsymbol{q}} + \boldsymbol{b}(\boldsymbol{q},\dot{\boldsymbol{q}}) + \boldsymbol{g}(\boldsymbol{q}) \tag{2}$$

where $\boldsymbol{\tau}$ is the $n \times 1$ vector of generalized actuator forces (torques) and $\boldsymbol{g}(\boldsymbol{q})$ is the $n \times 1$ vector of gravity terms. The form of (2) assumes that the generalized actuator forces can be directly interpreted as control inputs; that is, $\boldsymbol{\tau} = \boldsymbol{B}^T\boldsymbol{u} = \boldsymbol{u}$, ie. $\boldsymbol{B}^T = \mathbf{1}$. Additionally, the generalized applied forces are assumed to be restricted to gravity terms; that is, $\boldsymbol{f}(\boldsymbol{q},\dot{\boldsymbol{q}}) = -\boldsymbol{g}(\boldsymbol{q})$. This second assumption is relatively minor and will not limit the generality of the approaches presented in this paper. The first assumption regarding the control inputs restricts our examination to fully actuated systems. However, this limitation can be overcome by introducing a selection matrix (similar to $\boldsymbol{B}^T$ in mapping actuator control inputs to generalized actuator forces). We utilize this for a partial examination of under-actuated systems in *Section 5*.

2.2 Multiplier Form of the System Dynamics

We introduce a set of m_C holonomic and scleronomic constraint equations, $\boldsymbol{\phi}(\boldsymbol{q}) = \mathbf{0}$, that are satisfied on a $p = n - m_C$ dimensional manifold, Q^p, in configuration space, $Q = \mathbb{R}^n$. The gradient of $\boldsymbol{\phi}$ yields the $m_C \times n$ constraint Jacobian matrix, $\boldsymbol{\Phi}$. Adjoining the constraints to (2) by introducing a set of constraint forces yields the dynamic equation,

$$\boldsymbol{\tau} = \boldsymbol{M}\ddot{\boldsymbol{q}} + \boldsymbol{b} + \boldsymbol{g} - \boldsymbol{\tau}_C \tag{3}$$

subject to,

$$\boldsymbol{\Phi}\ddot{\boldsymbol{q}} + \dot{\boldsymbol{\Phi}}\dot{\boldsymbol{q}} = \mathbf{0} \qquad (\boldsymbol{\phi} = \mathbf{0}, \quad \boldsymbol{\Phi}\dot{\boldsymbol{q}} = \mathbf{0}) \tag{4}$$

where $\boldsymbol{\tau}_C$ is the vector of generalized constraint forces. The variation of the constraint equations yields $\delta\boldsymbol{\phi}(\boldsymbol{q}) = \boldsymbol{\Phi}\,\delta\boldsymbol{q} = \mathbf{0}$, which implies $\delta\boldsymbol{q} \in \ker(\boldsymbol{\Phi})$. The operator *ker()* represents the *kernel* of a matrix and in this context will be synonymous with the *null space* of a matrix throughout this paper. Since the constraints do no virtual work under these constraint consistent virtual displacements we have,

$$\boldsymbol{\tau}_C \perp \delta\boldsymbol{q} \qquad \forall\, \delta\boldsymbol{q} \in \ker(\boldsymbol{\Phi}) \tag{5}$$

The $\ker(\boldsymbol{\Phi})$ represents the tangent space of the constrained motion manifold, Q^p, at a point, $\boldsymbol{q}$, in configuration space. The constraint consistent virtual displacements, $\delta\boldsymbol{q}$, lie in this tangent space and the generalized constraint forces, $\boldsymbol{\tau}_C$, are orthogonal to it. This is illustrated in *Figure 3*. Based on this, the following is implied,

$$\boldsymbol{\tau}_C \in \ker(\boldsymbol{\Phi})^{\perp} = \mathrm{im}(\boldsymbol{\Phi}^T) \tag{6}$$

where the operator *im()* represents the *image* of a matrix and in this context will be synonymous with the *range* of a matrix throughout this paper.

Thus, the generalized constraint force can be represented as a linear combination of the columns of $\boldsymbol{\Phi}^T$. That is, $\boldsymbol{\tau}_C = \boldsymbol{\Phi}^T\boldsymbol{\lambda}$, where $\boldsymbol{\lambda}$ is a vector of unknown Lagrange multipliers. The constrained multibody equations of motion, expressed in the familiar multiplier form, are thus,

$$\boldsymbol{\tau} = \boldsymbol{M}\ddot{\boldsymbol{q}} + \boldsymbol{b} + \boldsymbol{g} - \boldsymbol{\Phi}^T\boldsymbol{\lambda} \tag{7}$$

subject to (4).

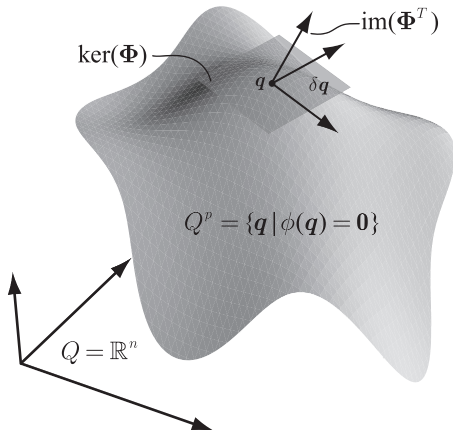

Figure 3: The configuration space constrained motion manifold, Q^p. All constraint consistent virtual variations, $\delta\boldsymbol{q}$, lie in the tangent space of Q^p and are orthogonal to the constraint forces.

2.3 Elimination of Multipliers

The Lagrange multipliers can be eliminated from (7) by first expressing the zeroth order variational equation,

$$\boldsymbol{\tau}_C \cdot \delta\boldsymbol{q} + (\boldsymbol{\tau} - \boldsymbol{M}\ddot{\boldsymbol{q}} - \boldsymbol{b} - \boldsymbol{g}) \cdot \delta\boldsymbol{q} = 0 \tag{8}$$

By restricting the variations to constraint consistent virtual displacements we have,

$$\begin{gathered} \boldsymbol{\tau}_C \cdot \delta\boldsymbol{q} + (\boldsymbol{\tau} - \boldsymbol{M}\ddot{\boldsymbol{q}} - \boldsymbol{b} - \boldsymbol{g}) \cdot \delta\boldsymbol{q} = 0 \\ \forall\, \delta\boldsymbol{q} \in \ker(\boldsymbol{\Phi}) \end{gathered} \tag{9}$$

Recalling (5) we note that the generalized constraint forces produce no virtual work under virtual displacements that are consistent with the constraints. Thus, the term $\boldsymbol{\tau}_C \cdot \delta\boldsymbol{q}$ vanishes from (9) and we have the following orthogonality relation,

$$\begin{gathered} (\boldsymbol{M}\ddot{\boldsymbol{q}} + \boldsymbol{b} + \boldsymbol{g} - \boldsymbol{\tau}) \cdot \delta\boldsymbol{q} = 0 \\ \forall\, \delta\boldsymbol{q} \in \ker(\boldsymbol{\Phi}) \end{gathered} \tag{10}$$

We now define a matrix, $\boldsymbol{C} \in \mathbb{R}^{n \times p}$, whose columns span the null space of $\boldsymbol{\Phi}$. This implies that $\mathrm{im}(\boldsymbol{C}) = \ker(\boldsymbol{\Phi})$. Thus, $\boldsymbol{\Phi}\boldsymbol{C} = \boldsymbol{0}$ and $\boldsymbol{C}^T\boldsymbol{\Phi}^T = \boldsymbol{0}$. In this manner $\boldsymbol{C}$ orthogonally complements $\boldsymbol{\Phi}$. That is,

$$\mathrm{im}(\boldsymbol{C}) = \ker(\boldsymbol{\Phi}) = \mathrm{im}(\boldsymbol{\Phi}^T)^{\perp} \tag{11}$$

Geometrically, $\mathrm{im}(\boldsymbol{C})$ represents the tangent space of the constrained motion manifold, Q^p (see *Figure 3*). These geometric properties are discussed in further detail in [2][14]. While not required for the subsequent analysis we specify that the columns of $\boldsymbol{C}$ be mutually orthogonal and thus form an orthogonal basis, $\mathcal{C}$, for the null space of $\boldsymbol{\Phi}$. The constraint consistent virtual displacements, $\delta\boldsymbol{q} \in \ker(\boldsymbol{\Phi})$, can then be expressed in terms of the virtual displacements of a minimal set of p independent coordinates, $\boldsymbol{q}_p$,

$$\delta \boldsymbol{q} = \boldsymbol{C}\, \delta \boldsymbol{q}_p \tag{12}$$

Using this relationship we can express (10) over all possible variations of a minimal set of coordinates,

$$\begin{gathered}(\boldsymbol{C}^T \boldsymbol{M} \ddot{\boldsymbol{q}} + \boldsymbol{C}^T \boldsymbol{b} + \boldsymbol{C}^T \boldsymbol{g} - \boldsymbol{C}^T \boldsymbol{\tau}) \cdot \delta \boldsymbol{q}_p = 0 \\ \forall\, \delta \boldsymbol{q}_p \in \mathbb{R}^p \\ \Downarrow \\ \boldsymbol{C}^T \boldsymbol{\tau} = \boldsymbol{C}^T \boldsymbol{M} \ddot{\boldsymbol{q}} + \boldsymbol{C}^T \boldsymbol{b} + \boldsymbol{C}^T \boldsymbol{g}\end{gathered} \tag{13}$$

Noting that $\dot{\boldsymbol{q}} = \boldsymbol{C}\dot{\boldsymbol{q}}_p$ and $\ddot{\boldsymbol{q}} = \boldsymbol{C}\ddot{\boldsymbol{q}}_p + \dot{\boldsymbol{C}}\dot{\boldsymbol{q}}_p$ we can express (13) as,

$$\boldsymbol{\tau}_p = \boldsymbol{M}_p(\boldsymbol{q})\, \ddot{\boldsymbol{q}}_p + \boldsymbol{b}_p(\boldsymbol{q}, \dot{\boldsymbol{q}}_p) + \boldsymbol{g}_p(\boldsymbol{q}) \tag{14}$$

where,

$$\begin{aligned}\boldsymbol{M}_p(\boldsymbol{q}) &= \boldsymbol{C}^T \boldsymbol{M} \boldsymbol{C} \\ \boldsymbol{b}_p(\boldsymbol{q}, \dot{\boldsymbol{q}}_p) &= \boldsymbol{C}^T \boldsymbol{b} + \boldsymbol{C}^T \boldsymbol{M} \dot{\boldsymbol{C}} \dot{\boldsymbol{q}}_p \\ \boldsymbol{g}_p(\boldsymbol{q}) &= \boldsymbol{C}^T \boldsymbol{g} \\ \boldsymbol{\tau}_p &= \boldsymbol{C}^T \boldsymbol{\tau}\end{aligned} \tag{15}$$

The approach outlined here is well known in multibody dynamics and is consistent with the projection method of [2]. This approach was also used by Russakow et al. for application to serial-to-parallel chain manipulators [25]. We note that (14) includes a mix of our initial set of n generalized coordinates, $\boldsymbol{q}$, as well as the minimal set of p independent coordinates, $\boldsymbol{q}_p$. Since the constraints are holonomic we would expect there to be a mapping, in principle, which could be derived from the constraints that would yield $\boldsymbol{q} = \boldsymbol{q}(\boldsymbol{q}_p)$. In this case $\boldsymbol{C}$ could be computed explicitly from the mapping rather than computing the null space of $\boldsymbol{\Phi}$; that is, $\boldsymbol{C} = \partial \boldsymbol{q} / \partial \boldsymbol{q}_p$. Additionally, the terms in (14) could be expressed as functions of $\boldsymbol{q}_p$ rather than $\boldsymbol{q}$. Since $\boldsymbol{q}_p$ are independent coordinates the constraints would be implicitly addressed and the resulting system would be unconstrained with respect to configuration space. However, finding the mapping $\boldsymbol{q} = \boldsymbol{q}(\boldsymbol{q}_p)$ would be difficult in general. In such cases a null space method or a coordinate partitioning method [29] would need to be used to compute $\boldsymbol{C}$.

Additionally, the generalized coordinates, $\boldsymbol{q}_p$, and the generalized forces, $\boldsymbol{\tau}_p$, do not necessarily have a natural and physically intuitive meaning, making it difficult to standardize their use in a numerical algorithm. This is in contrast to the coordinates, $\boldsymbol{q}$, which are chosen specifically to describe the system in the most natural and physically intuitive manner. It is usually desirable to select $\boldsymbol{q}$ in a manner that preserves the physical meaning of the generalized forces as torques about individual joints. Often when using a minimal set of coordinates this is not the case, since a single generalized coordinate may influence multiple joint displacements. Therefore, from an algorithmic perspective it is often preferable to deal with a non-minimal but standardized set of generalized coordinates (like joint angles) that are amenable to numerical formulation, and compute the dynamic terms corresponding to that kinematic parametrization. Equation (14) can then be used, as is, parameterized in terms of $\boldsymbol{q}$.

2.4 Minimization Form of the System Dynamics

By expressing the zeroth order variational equation (9) we arrive at an orthogonality relation (10). Higher order variations yield similar orthogonality relations. In the particular case of second order variations, known as virtual accelerations, we can arrive at a minimization principle. This was first demonstrated by Gauss [9] and later investigated by Gibbs [10] in modified form. We begin by first expressing the second order variational form of (3),

$$\boldsymbol{\tau}_C \cdot \delta\ddot{\boldsymbol{q}} + (\boldsymbol{\tau} - \boldsymbol{M}\ddot{\boldsymbol{q}} - \boldsymbol{b} - \boldsymbol{g}) \cdot \delta\ddot{\boldsymbol{q}} = 0 \tag{16}$$

The virtual accelerations, $\delta\ddot{\boldsymbol{q}}$, refer to all acceleration variations which satisfy the constraints while time, position, and velocity are fixed. Since we are assuming scleronomic constraints we only need to be concerned with position and velocity remaining fixed. Given $\delta\boldsymbol{q} = \boldsymbol{0}$ and $\delta\dot{\boldsymbol{q}} = \boldsymbol{0}$ the variation of (4) yields,

$$\delta(\boldsymbol{\Phi}\ddot{\boldsymbol{q}} + \dot{\boldsymbol{\Phi}}\dot{\boldsymbol{q}}) = \boldsymbol{\Phi}\,\delta\ddot{\boldsymbol{q}} = \boldsymbol{0} \tag{17}$$

which implies that $\delta\ddot{\boldsymbol{q}} \in \ker(\boldsymbol{\Phi})$. Under this condition (16) can be restricted to constraint consistent virtual accelerations,

$$\begin{gathered} \boldsymbol{\tau}_C \cdot \delta\ddot{\boldsymbol{q}} + (\boldsymbol{\tau} - \boldsymbol{M}\ddot{\boldsymbol{q}} - \boldsymbol{b} - \boldsymbol{g}) \cdot \delta\ddot{\boldsymbol{q}} = 0 \\ \forall\, \delta\ddot{\boldsymbol{q}} \in \ker(\boldsymbol{\Phi}) \end{gathered} \tag{18}$$

Recalling (5) we have,

$$\boldsymbol{\tau}_C \perp \delta\ddot{\boldsymbol{q}} \qquad \forall\, \delta\ddot{\boldsymbol{q}} \in \ker(\boldsymbol{\Phi}) \tag{19}$$

Thus the term $\boldsymbol{\tau}_C \cdot \delta\ddot{\boldsymbol{q}}$ vanishes from (18) and we have the following orthogonality relation,

$$\begin{gathered} (\boldsymbol{M}\ddot{\boldsymbol{q}} + \boldsymbol{b} + \boldsymbol{g} - \boldsymbol{\tau}) \cdot \delta\ddot{\boldsymbol{q}} = 0 \\ \forall\, \delta\ddot{\boldsymbol{q}} \in \ker(\boldsymbol{\Phi}) \end{gathered} \tag{20}$$

subject to (4). At this point we introduce the *Gauss function*, $\mathcal{G}$, defined as a mass-weighted distance measure between the constrained and unconstrained accelerations,

$$\mathcal{G} \triangleq \frac{1}{2}(\ddot{\boldsymbol{q}} - \ddot{\boldsymbol{q}}_\star)^T \boldsymbol{M} (\ddot{\boldsymbol{q}} - \ddot{\boldsymbol{q}}_\star) \tag{21}$$

where $\ddot{\boldsymbol{q}}_\star$ is the *unconstrained acceleration* of the system. That is, $\ddot{\boldsymbol{q}}_\star$ is the generalized acceleration that the system would exhibit in the absence of constraints,

$$\ddot{\boldsymbol{q}}_\star = \boldsymbol{M}^{-1}(\boldsymbol{\tau} - \boldsymbol{b} - \boldsymbol{g}) \tag{22}$$

Taking the gradient of $\mathcal{G}$ with respect to $\ddot{\boldsymbol{q}}$ yields,

$$\frac{\partial \mathcal{G}}{\partial \ddot{\boldsymbol{q}}} = \boldsymbol{M}(\ddot{\boldsymbol{q}} - \ddot{\boldsymbol{q}}_\star) = \boldsymbol{M}\ddot{\boldsymbol{q}} + \boldsymbol{b} + \boldsymbol{g} - \boldsymbol{\tau} \tag{23}$$

Substituting (23) into (20) yields,

$$\frac{\partial \mathcal{G}}{\partial \ddot{\boldsymbol{q}}} \cdot \delta\ddot{\boldsymbol{q}} = 0 \qquad\qquad \forall\, \delta\ddot{\boldsymbol{q}} \in \ker(\boldsymbol{\Phi}) \tag{24}$$

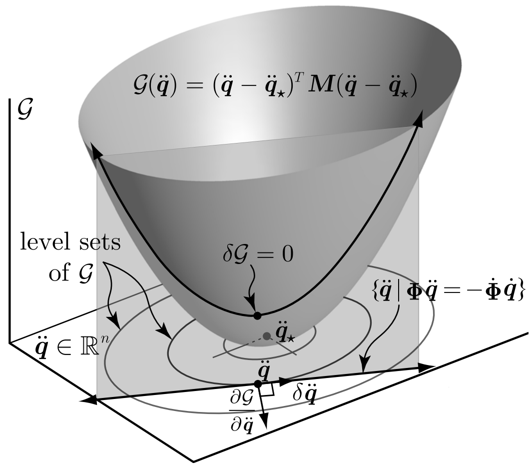

Figure 4: The Gauss function, $\mathcal{G}$, is minimized subject to the constraints. At the solution point, $\ddot{\boldsymbol{q}}$, the gradient of $\mathcal{G}$ is orthogonal to the space of virtual accelerations. Geometrically, the solution minimizes the distance (mass-weighted) to the unconstrained acceleration, $\ddot{\boldsymbol{q}}_\star$.

This implies that the solution of the constrained multibody dynamics problem yields a stationary value of $\mathcal{G}$ over the set of constraint consistent accelerations, or,

$$\delta\mathcal{G} = 0 \qquad \forall\, \delta \,|\, \delta\ddot{\boldsymbol{q}} \in \ker(\boldsymbol{\Phi}) \tag{25}$$

subject to (4). This is illustrated geometrically in *Figure 4* and expresses *Gauss' Principle of Least Constraint* [4] [24] [28]. These conditions require that the actual generalized acceleration, $\ddot{\boldsymbol{q}}$, result in a stationary value of the Gauss function, $\mathcal{G}$, and be consistent with the constraints. Moreover, since $\mathcal{G}$ is a quadratic form and $\boldsymbol{M}$ is symmetric positive definite, $\ddot{\boldsymbol{q}}$ must *minimize* $\mathcal{G}$ subject to the constraints.

2.5 Solution of the Constrained Dynamics Problem

As we have seen, the problem of constrained multibody dynamics can be stated as a multiplier problem or a minimization problem. Both of these statements are equivalent. That is, the solution of the multiplier problem minimizes the Gauss function, $\mathcal{G}$, over the set of constraint consistent accelerations and the solution of the minimization problem satisfies the multiplier equations.

We can arrive at an explicit solution of the constrained dynamics problem. Using (22) we can express (7) and (4) as,

$$\begin{aligned} \boldsymbol{M}(\ddot{\boldsymbol{q}} - \ddot{\boldsymbol{q}}_\star) &= \boldsymbol{\Phi}^T\boldsymbol{\lambda} \\ \boldsymbol{\Phi}\ddot{\boldsymbol{q}} + \dot{\boldsymbol{\Phi}}\dot{\boldsymbol{q}} &= \boldsymbol{0} \end{aligned} \tag{26}$$

It is straightforward to solve this system. The solution yields,

$$\begin{aligned} \ddot{\boldsymbol{q}} &= -\boldsymbol{M}^{-1}\boldsymbol{\Phi}^T(\boldsymbol{\Phi}\boldsymbol{M}^{-1}\boldsymbol{\Phi}^T)^{-1}(\boldsymbol{\Phi}\ddot{\boldsymbol{q}}_\star + \dot{\boldsymbol{\Phi}}\dot{\boldsymbol{q}}) + \ddot{\boldsymbol{q}}_\star \\ \boldsymbol{\lambda} &= -(\boldsymbol{\Phi}\boldsymbol{M}^{-1}\boldsymbol{\Phi}^T)^{-1}(\boldsymbol{\Phi}\ddot{\boldsymbol{q}}_\star + \dot{\boldsymbol{\Phi}}\dot{\boldsymbol{q}}) \end{aligned} \tag{27}$$

We now express the mass-weighted (right) inverse of $\mathbf{\Phi}$,

$$\bar{\mathbf{\Phi}} = \boldsymbol{M}^{-1}\mathbf{\Phi}^T(\mathbf{\Phi}\boldsymbol{M}^{-1}\mathbf{\Phi}^T)^{-1} \tag{28}$$

where $\mathbf{\Phi}\bar{\mathbf{\Phi}} = \mathbf{1}$ and, equivalently, $\bar{\mathbf{\Phi}}^T\mathbf{\Phi}^T = \mathbf{1}$. We then have,

$$\ddot{\boldsymbol{q}} = -\bar{\mathbf{\Phi}}\dot{\mathbf{\Phi}}\dot{\boldsymbol{q}} + (\mathbf{1} - \bar{\mathbf{\Phi}}\mathbf{\Phi})\ddot{\boldsymbol{q}}_\star \tag{29}$$

Defining the $n \times n$ constraint null space matrix, $\mathbf{\Theta} \triangleq \mathbf{1} - \bar{\mathbf{\Phi}}\mathbf{\Phi}$, we can write,

$$\ddot{\boldsymbol{q}} = -\bar{\mathbf{\Phi}}\dot{\mathbf{\Phi}}\dot{\boldsymbol{q}} + \mathbf{\Theta}\ddot{\boldsymbol{q}}_\star \tag{30}$$

Since this solution satisfies Gauss' Principle we know that it minimizes $\mathcal{G}$ while satisfying the constraints. The mass weighted inverse, $\bar{\mathbf{\Phi}}$, of the constraint matrix therefore yields the solution of (4) which minimizes $\mathcal{G}$.

It is noted that $\mathbf{\Phi}$ and $\mathbf{\Theta}$ satisfy the condition $\mathbf{\Phi}\mathbf{\Theta} = \mathbf{0}$ and, equivalently, $\mathbf{\Theta}^T\mathbf{\Phi}^T = \mathbf{0}$. Further, if we form the projection matrix $\boldsymbol{P}^T = \boldsymbol{P}$ which projects any vector in $\mathbb{R}^n$ onto the null space of $\mathbf{\Phi}$ we have,

$$\boldsymbol{P}^T = \boldsymbol{C}\boldsymbol{C}^T = \mathbf{1} - \mathbf{\Phi}^T(\mathbf{\Phi}\mathbf{\Phi}^T)^{-1}\mathbf{\Phi} \tag{31}$$

where $\boldsymbol{C}$ is the matrix, defined in *Section 2.3*, which spans the null space of $\mathbf{\Phi}$. The expression for $\boldsymbol{P}^T$ in (31) has a similar form as the expression,

$$\mathbf{\Theta}^T = \mathbf{1} - \bar{\mathbf{\Phi}}\mathbf{\Phi} = \mathbf{1} - \mathbf{\Phi}^T(\mathbf{\Phi}\boldsymbol{M}^{-1}\mathbf{\Phi}^T)^{-1}\mathbf{\Phi}\boldsymbol{M}^{-1} \tag{32}$$

Consequently $\boldsymbol{P}^T = \boldsymbol{C}\boldsymbol{C}^T$ can be regarded as a *kinematic* constraint null space projection matrix and $\mathbf{\Theta}^T$ can be regarded as a *mass-weighted* constraint null space projection matrix. The physical and geometric meaning of $\mathbf{\Phi}$ and $\mathbf{\Theta}$ will be discussed further in *Section 4*.

2.6 Generalized Constrained Equation of Motion

Given the explicit solution of the constrained dynamics problem (27) we now wish to express an alternate form of the constrained dynamical equations of motion. We begin by expressing $\boldsymbol{\lambda}$ in (27) as,

$$\boldsymbol{\lambda} = -\mathbf{H}[\mathbf{\Phi}\boldsymbol{M}^{-1}(\boldsymbol{\tau} - \boldsymbol{b} - \boldsymbol{g}) + \dot{\mathbf{\Phi}}\dot{\boldsymbol{q}}] \tag{33}$$

where $\mathbf{H}$ is the $m_C \times m_C$ constraint space mass matrix which reflects the system inertia projected at the constraint,

$$\mathbf{H} \triangleq (\mathbf{\Phi}\boldsymbol{M}^{-1}\mathbf{\Phi}^T)^{-1} \tag{34}$$

Substituting (33) into (7) yields,

$$\boldsymbol{M}\ddot{\boldsymbol{q}} + \boldsymbol{b} + \boldsymbol{g} = -\mathbf{\Phi}^T\mathbf{H}\dot{\mathbf{\Phi}}\dot{\boldsymbol{q}} + (\mathbf{1} - \mathbf{\Phi}^T\mathbf{H}\mathbf{\Phi}\boldsymbol{M}^{-1})\boldsymbol{\tau} + \mathbf{\Phi}^T\mathbf{H}\mathbf{\Phi}\boldsymbol{M}^{-1}(\boldsymbol{b} + \boldsymbol{g}) \tag{35}$$

We now define the $m_C \times 1$ vector of centrifugal and Coriolis forces projected at the constraint,

$$\boldsymbol{\alpha} \triangleq \mathbf{H}\mathbf{\Phi}\boldsymbol{M}^{-1}\boldsymbol{b} - \mathbf{H}\dot{\mathbf{\Phi}}\dot{\boldsymbol{q}} \tag{36}$$

and the $m_C \times 1$ vector of gravity forces projected at the constraint,

$$\boldsymbol{\rho} \triangleq \mathbf{H}\boldsymbol{\Phi}\boldsymbol{M}^{-1}\boldsymbol{g} \tag{37}$$

We also note that,

$$\boldsymbol{\Theta}^T = \mathbf{1} - \boldsymbol{\Phi}^T\bar{\boldsymbol{\Phi}}^T = \mathbf{1} - \boldsymbol{\Phi}^T\mathbf{H}\boldsymbol{\Phi}\boldsymbol{M}^{-1} \tag{38}$$

Substituting these expressions into (35) we have the concise expression which we will refer to as the *generalized constrained equation of motion*,

$$\boldsymbol{\Theta}^T\boldsymbol{\tau} = \boldsymbol{M}\ddot{\boldsymbol{q}} + \boldsymbol{b} + \boldsymbol{g} - \boldsymbol{\Phi}^T(\boldsymbol{\alpha} + \boldsymbol{\rho}) \tag{39}$$

An alternative means of deriving this equation involves directly mapping the configuration space equation (7) into the constraint null space using $\boldsymbol{\Theta}^T$,

$$\boldsymbol{\Theta}^T\boldsymbol{\tau} = \boldsymbol{\Theta}^T\boldsymbol{M}\ddot{\boldsymbol{q}} + \boldsymbol{\Theta}^T\boldsymbol{b} + \boldsymbol{\Theta}^T\boldsymbol{g} - \boldsymbol{\Theta}^T\boldsymbol{\Phi}^T\boldsymbol{\lambda} \tag{40}$$

Noting that $\boldsymbol{\Theta}^T\boldsymbol{\Phi}^T = \mathbf{0}$ and manipulating we have,

$$\begin{aligned}\boldsymbol{\Theta}^T\boldsymbol{\tau} &= \boldsymbol{M}\ddot{\boldsymbol{q}} + \boldsymbol{b} + \boldsymbol{g} - \boldsymbol{\Phi}^T\bar{\boldsymbol{\Phi}}^T\boldsymbol{M}\ddot{\boldsymbol{q}} - \boldsymbol{\Phi}^T\bar{\boldsymbol{\Phi}}^T\boldsymbol{b} - \boldsymbol{\Phi}^T\bar{\boldsymbol{\Phi}}^T\boldsymbol{g} \\ &= \boldsymbol{M}\ddot{\boldsymbol{q}} + \boldsymbol{b} + \boldsymbol{g} - \boldsymbol{\Phi}^T\mathbf{H}\boldsymbol{\Phi}\ddot{\boldsymbol{q}} - \boldsymbol{\Phi}^T(\boldsymbol{\alpha} + \boldsymbol{\rho}) - \boldsymbol{\Phi}^T\mathbf{H}\dot{\boldsymbol{\Phi}}\dot{\boldsymbol{q}}\end{aligned} \tag{41}$$

Substituting in our constraint condition, $\dot{\boldsymbol{\Phi}}\dot{\boldsymbol{q}} = -\boldsymbol{\Phi}\ddot{\boldsymbol{q}}$, yields,

$$\boldsymbol{\Theta}^T\boldsymbol{\tau} = \boldsymbol{M}\ddot{\boldsymbol{q}} + \boldsymbol{b} + \boldsymbol{g} - \boldsymbol{\Phi}^T(\boldsymbol{\alpha} + \boldsymbol{\rho}) \tag{42}$$

3 Task Space Dynamics

In the previous section we considered configuration space descriptions of the dynamics of constrained multibody systems. Our objective is to reformulate these descriptions in the context of task space. This will provide the foundation for constrained task-level control to be discussed in the next section. As a starting point we begin with a review of the basic operational space framework [15] [16].

The operational space framework addresses the dynamics and control of branching chain robots. Given a branching chain system the initial step involves defining a set of m_T task, or operational space, coordinates, $\boldsymbol{x}$. The function $\boldsymbol{x}(\boldsymbol{q})$ represents a kinematic mapping from the set of generalized coordinates to the set of operational space coordinates. The operational space coordinates can represent any function of the generalized coordinates but typically are chosen to describe the set of control coordinates associated with a motion control task. *Figure 5* illustrates simple branching chain systems where the operational space coordinates are chosen to be the Cartesian coordinates associated with positioning the terminal point(s) of the chain. Further, by taking the gradient of $\mathbf{x}$ we have the relationship,

$$\dot{\boldsymbol{x}} = \boldsymbol{J}(\boldsymbol{q})\,\dot{\boldsymbol{q}} \tag{43}$$

where $\boldsymbol{J}(\boldsymbol{q})$ is the $m_T \times n$ task Jacobian matrix. This relationship applies to both kinematically non-redundant and redundant systems. In the case of non-redundant

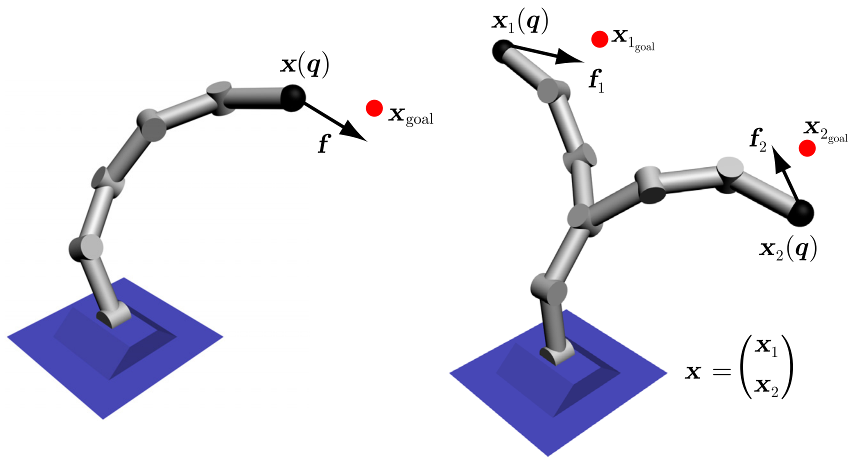

Figure 5: (Left) A simple task description for a serial chain where the operational space coordinates describe the Cartesian position of the terminal point of the chain. (Right) A branching chain where the operational space coordinates describe the positions of both terminal points.

systems the inverse of this relationship is well defined outside of singularities. For such cases we have,

$$\dot{\boldsymbol{q}} = \boldsymbol{J}^{-1}\dot{\mathbf{x}} \tag{44}$$

In the redundant case we can define the right inverse of $\boldsymbol{J}$ as,

$$\{\boldsymbol{J}^{\#} \,|\, \boldsymbol{J}\boldsymbol{J}^{\#} = \mathbf{1}\} \tag{45}$$

The solutions to $\boldsymbol{J}\dot{\boldsymbol{q}} = \dot{\mathbf{x}}$ are thus given by,

$$\dot{\boldsymbol{q}} = \boldsymbol{J}^{\#}\dot{\mathbf{x}} + \boldsymbol{N}\dot{\boldsymbol{q}}_o \tag{46}$$

where $\boldsymbol{N} \triangleq \mathbf{1} - \boldsymbol{J}^{\#}\boldsymbol{J}$ and $\boldsymbol{q}_o$ is an arbitrary vector in $\mathbb{R}^n$.

At this point we can address operational space kinetics. In the non-redundant case any generalized force can be produced by an operational space force, $\boldsymbol{f}$, acting at the task point along the task coordinates. *Figure 5* illustrates the action of the operational space force for the intuitive case of Cartesian positioning tasks. The generalized force is then composed as $\boldsymbol{J}^T\boldsymbol{f}$. In the redundant case an additional term needs to complement the task term in order to realize any arbitrary generalized force. We will refer to this term as the null space term and it can be composed as $\boldsymbol{N}^T\boldsymbol{\tau}_o$, where $\boldsymbol{N}^T$ is the null space projection matrix. An arbitrary generalized force, $\boldsymbol{\tau}$, can then be expressed as,

$$\boldsymbol{\tau} = \boldsymbol{J}^T\boldsymbol{f} + \boldsymbol{N}^T\boldsymbol{\tau}_o = \boldsymbol{M}\ddot{\boldsymbol{q}} + \boldsymbol{b} + \boldsymbol{g} \tag{47}$$

We can pre-multiply (47) by $\boldsymbol{J}\boldsymbol{M}^{-1}$ and rearrange to get,

$$\ddot{\mathbf{x}} = \boldsymbol{J}\boldsymbol{M}^{-1}\boldsymbol{J}^T\boldsymbol{f} + \boldsymbol{J}\boldsymbol{M}^{-1}\boldsymbol{N}^T\boldsymbol{\tau}_o - \boldsymbol{J}\boldsymbol{M}^{-1}\boldsymbol{b} - \boldsymbol{J}\boldsymbol{M}^{-1}\boldsymbol{g} + \dot{\boldsymbol{J}}\dot{\boldsymbol{q}} \tag{48}$$

where we note that $\ddot{\mathbf{x}} = \boldsymbol{J}\ddot{\boldsymbol{q}} + \dot{\boldsymbol{J}}\dot{\boldsymbol{q}}$. We can now impose the condition that the term associated with the null space, $\boldsymbol{N}^T\boldsymbol{\tau}_o$, does not contribute to the operational space acceleration. This is referred to as *dynamic consistency* [16] and is expressed as,

$$\boldsymbol{J}\boldsymbol{M}^{-1}\boldsymbol{N}^T\boldsymbol{\tau}_o = \boldsymbol{J}\boldsymbol{M}^{-1}(\mathbf{1} - \boldsymbol{J}^T\boldsymbol{J}^{T\#})\boldsymbol{\tau}_o = \mathbf{0}, \qquad \forall\,\boldsymbol{\tau}_o \in \mathbb{R}^n \tag{49}$$

We can solve for $\boldsymbol{J}^{\#}$ under this condition and denote this solution as $\bar{\boldsymbol{J}}$, the dynamically consistent (right) inverse of $\boldsymbol{J}$ [16],

$$\bar{\boldsymbol{J}} = \boldsymbol{M}^{-1}\boldsymbol{J}^T(\boldsymbol{J}\boldsymbol{M}^{-1}\boldsymbol{J}^T)^{-1} \tag{50}$$

This represents a unique right inverse of $\boldsymbol{J}$ where, by construction, the null space projection matrix, $\boldsymbol{N}^T = \mathbf{1} - \boldsymbol{J}^T\bar{\boldsymbol{J}}^T$, is guaranteed not to influence the task acceleration. Under this condition we can manipulate (48) to arrive at,

$$\begin{aligned}\boldsymbol{f} = (\boldsymbol{J}\boldsymbol{M}^{-1}\boldsymbol{J}^T)^{-1}\ddot{\mathbf{x}} + (\boldsymbol{J}\boldsymbol{M}^{-1}\boldsymbol{J}^T)^{-1}(\boldsymbol{J}\boldsymbol{M}^{-1}\boldsymbol{b} - \dot{\boldsymbol{J}}\dot{\boldsymbol{q}})\\ +(\boldsymbol{J}\boldsymbol{M}^{-1}\boldsymbol{J}^T)^{-1}\boldsymbol{J}\boldsymbol{M}^{-1}\boldsymbol{g}\end{aligned} \tag{51}$$

This expresses the operational space dynamical equation,

$$\boldsymbol{f} = \boldsymbol{\Lambda}(\boldsymbol{q})\,\ddot{\mathbf{x}} + \boldsymbol{\mu}(\boldsymbol{q},\dot{\boldsymbol{q}}) + \boldsymbol{p}(\boldsymbol{q}) \tag{52}$$

where $\boldsymbol{\Lambda}(\boldsymbol{q})$ is the $m_T \times m_T$ operational space mass matrix, $\boldsymbol{\mu}(\boldsymbol{q},\dot{\boldsymbol{q}})$ is the $m_T \times 1$ operational space centrifugal and Coriolis force vector, and $\boldsymbol{p}(\boldsymbol{q})$ is the $m_T \times 1$ operational space gravity vector.

$$\begin{aligned}\boldsymbol{\Lambda}(\boldsymbol{q}) &= (\boldsymbol{J}\boldsymbol{M}^{-1}\boldsymbol{J}^T)^{-1}\\ \boldsymbol{\mu}(\boldsymbol{q},\dot{\boldsymbol{q}}) &= \bar{\boldsymbol{J}}^T\boldsymbol{b}(\boldsymbol{q},\dot{\boldsymbol{q}}) - \boldsymbol{\Lambda}\dot{\boldsymbol{J}}\dot{\boldsymbol{q}}\\ \boldsymbol{p}(\boldsymbol{q}) &= \bar{\boldsymbol{J}}^T\boldsymbol{g}(\boldsymbol{q})\\ \bar{\boldsymbol{J}}^T &= \boldsymbol{\Lambda}\boldsymbol{J}\boldsymbol{M}^{-1}\end{aligned} \tag{53}$$

Thus, the overall dynamics of our multibody system can be mapped into task space using $\bar{\boldsymbol{J}}^T$,

$$\boldsymbol{\tau} = \boldsymbol{M}\ddot{\boldsymbol{q}} + \boldsymbol{b} + \boldsymbol{g} \quad \overset{\bar{\boldsymbol{J}}^T}{\rightarrow} \quad \boldsymbol{f} = \boldsymbol{\Lambda}\,\ddot{\mathbf{x}} + \boldsymbol{\mu} + \boldsymbol{p} \tag{54}$$

In a complementary manner the overall dynamics can be mapped into the task consistent null space (or self-motion space) using $\boldsymbol{N}^T$.

We can design the control for our system in task space coordinates using (52). Additionally, we can specify the null space behavior of our system with the term $\boldsymbol{N}^T\boldsymbol{\tau}_o$. The null space control term is guaranteed not to interfere with the task dynamics of (52) due to the condition of dynamic consistency. This allows for decoupled control design. Finally, the overall control torque applied to the system is composed as in (47).

4 Task and Constraint Symmetry

There are parallels between the structure of the constrained multibody dynamics problem, in both the multiplier and minimization forms, and the operational space formulation. These parallels are derived from the common mathematical description used for tasks and constraints. Both utilize a Jacobian representation (constraint matrix, $\boldsymbol{\Phi}$, or task Jacobian, $\boldsymbol{J}$).

Despite the common form used in specifying tasks and constraints, the mechanism by which tasks and constraints are satisfied differs. Tasks are *achieved* by means of a control input, whereas constraints are *imposed* by the physical structure of the multibody system. Nevertheless, due to their common mathematical form there are similarities between the structure of task dynamics and constrained dynamics.

Equation (39) provides a unique perspective into constrained dynamics. The projection matrix, $\boldsymbol{\Theta}^T$, filters out the component of the generalized force which acts in the direction of the constraint force. That is,

$$\boldsymbol{\Theta}^T \boldsymbol{\tau} = \boldsymbol{\tau} - \boldsymbol{\Phi}^T \bar{\boldsymbol{\Phi}}^T \boldsymbol{\tau} \tag{55}$$

Consequently, only the component of the generalized force which influences the motion of the system is preserved. Equivalent motion control [13] is produced by all choices of $\boldsymbol{\tau}$ which differ by a vector lying in the $\mathrm{im}(\boldsymbol{\Phi}^T)$. We also note that the complementary spaces defined by $\mathrm{im}(\boldsymbol{\Phi}^T)$ and $\mathrm{im}(\boldsymbol{\Theta}^T)$ are orthogonal in a mass-weighted sense,

$$\left\langle \boldsymbol{\Phi}^T, \boldsymbol{\Theta}^T \right\rangle_{M^{-1}} = \boldsymbol{\Phi} \boldsymbol{M}^{-1} \boldsymbol{\Theta}^T = \mathbf{0} \tag{56}$$

Similarly, the projection matrix, $\boldsymbol{N}^T$, filters out the component of the generalized force which produces acceleration in the task direction. That is,

$$\boldsymbol{N}^T \boldsymbol{\tau} = \boldsymbol{\tau} - \boldsymbol{J}^T \bar{\boldsymbol{J}}^T \boldsymbol{\tau} \tag{57}$$

Consequently, only the component of the generalized force which influences the internal self-motion of the system is preserved. We also note that the complementary spaces defined by $\mathrm{im}(\boldsymbol{J}^T)$ and $\mathrm{im}(\boldsymbol{N}^T)$ are orthogonal in a mass-weighted sense,

$$\left\langle \boldsymbol{J}^T, \boldsymbol{N}^T \right\rangle_{M^{-1}} = \boldsymbol{J} \boldsymbol{M}^{-1} \boldsymbol{N}^T = \mathbf{0} \tag{58}$$

To summarize, in the case of constrained motion a projection matrix, $\boldsymbol{\Theta}^T$, is used to project the overall dynamics into the constraint null space. This preserves only the dynamics which influences the constrained motion of the system. In the case of task space dynamics a projection matrix, $\boldsymbol{N}^T$, is used to project the overall dynamics into the task null space. This preserves only the dynamics which influences the task consistent self-motion of the system. In this respect tasks can be viewed as rheonomic servo (control) constraints [1] [3] [23] which enforce some motion control objective.

In addition to the symmetries between the constraint and task null space projection matrices there are properties shared by the constraint matrix and the task Jacobian with regard to the minimization of scalar “energy” measures (the Gauss function and the kinetic energy). Specifically, we can seek a solution to the kinematic relationship, $\boldsymbol{J}\dot{\boldsymbol{q}} = \dot{\boldsymbol{x}}$, which minimizes the kinetic energy,

$$T = \frac{1}{2} \dot{\boldsymbol{q}}^T \boldsymbol{M} \dot{\boldsymbol{q}} \tag{59}$$

The solution to this constrained minimization problem is straightforward and yields,

$$\dot{\boldsymbol{q}} = \boldsymbol{M}^{-1}\boldsymbol{J}^T(\boldsymbol{J}\boldsymbol{M}^{-1}\boldsymbol{J}^T)^{-1}\dot{\mathbf{x}} \tag{60}$$

Noting that the dynamically consistent inverse of $\boldsymbol{J}$ is given by,

$$\bar{\boldsymbol{J}} = \boldsymbol{M}^{-1}\boldsymbol{J}^T(\boldsymbol{J}\boldsymbol{M}^{-1}\boldsymbol{J}^T)^{-1} \tag{61}$$

we have that $\dot{\boldsymbol{q}} = \bar{\boldsymbol{J}}\dot{\boldsymbol{x}}$ yields the kinetic energy minimizing solution of (43).

Similarly, we can seek a solution of the acceleration expression,

$$\boldsymbol{J}\ddot{\boldsymbol{q}} = \ddot{\mathbf{x}} - \dot{\boldsymbol{J}}\dot{\boldsymbol{q}} \tag{62}$$

which minimizes the *acceleration energy*, defined as the following mass-weighted quadratic form,

$$\frac{1}{2}\ddot{\boldsymbol{q}}^T\boldsymbol{M}\ddot{\boldsymbol{q}} \tag{63}$$

This yields,

$$\ddot{\boldsymbol{q}} = \boldsymbol{M}^{-1}\boldsymbol{J}^T(\boldsymbol{J}\boldsymbol{M}^{-1}\boldsymbol{J}^T)^{-1}(\ddot{\mathbf{x}} - \dot{\boldsymbol{J}}\dot{\boldsymbol{q}}) \tag{64}$$

and we have that $\ddot{\boldsymbol{q}} = \bar{\boldsymbol{J}}(\ddot{\mathbf{x}} - \dot{\boldsymbol{J}}\dot{\boldsymbol{q}})$ yields the acceleration energy minimizing solution of (62).

The dynamically consistent inverse, $\bar{\boldsymbol{J}}$, of the task Jacobian therefore yields task consistent solutions which minimize both the kinetic energy and acceleration energy of the system. This is analogous to the manner in which the mass-weighted inverse, $\bar{\boldsymbol{\Phi}}$, of the constraint matrix yields a constraint consistent solution which minimizes the Gauss function.

The symmetry between constraint dynamics and task dynamics will be exploited for the purposes of control in the following section.

5 Constrained Task-Level Control

In previous work the control of constrained systems has been examined from a configuration space perspective, particularly with regard to contact control in robot manipulators [20][21]. We will present an operational space methodology for addressing constrained systems, thus providing a means of applying operational space control structures to these systems.

5.1 Direct Task Space Mapping of Constrained Dynamics

This formulation involves directly mapping the generalized constrained equation of motion (39) into operational space coordinates using the dynamically consistent inverse of the task Jacobian. Alternately, we will make use of the constrained equation of motion in which the Lagrange multipliers have been eliminated through the introduction of a minimal set of independent coordinates (14). As with (39) this equation can be directly mapped into operational space coordinates using the dynamically consistent inverse of the task Jacobian.

We begin by recalling the generalized constrained equation of motion (39),

$$\boldsymbol{\Theta}^T\boldsymbol{\tau} = \boldsymbol{M}\ddot{\boldsymbol{q}} + \boldsymbol{b} + \boldsymbol{g} - \boldsymbol{\Phi}^T(\boldsymbol{\alpha} + \boldsymbol{\rho}) \tag{65}$$

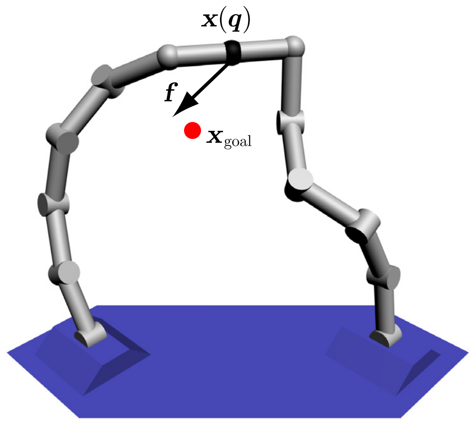

Figure 6: A multibody system with loop constraints. The task coordinates, $\mathbf{x}$, are assigned to a point on one of the links. The objective is to control the constrained system using task-level commands.

We can relate a set of task coordinates, $\mathbf{x}$, to the set of generalized coordinates, $\boldsymbol{q}$, by,

$$\dot{\mathbf{x}} = \boldsymbol{J}\dot{\boldsymbol{q}} \tag{66}$$

Mapping (65) into any appropriate task space via the dynamically consistent inverse of $\boldsymbol{J}$ yields,

$$\bar{\boldsymbol{J}}^T \boldsymbol{\Theta}^T \boldsymbol{\tau} = \boldsymbol{\Lambda}(\boldsymbol{q})\,\ddot{\mathbf{x}} + \boldsymbol{\mu}(\boldsymbol{q},\dot{\boldsymbol{q}}) + \boldsymbol{p}(\boldsymbol{q}) + \boldsymbol{\gamma}(\boldsymbol{q}) \tag{67}$$

where,

$$\begin{aligned} \boldsymbol{\Lambda}(\boldsymbol{q}) &= (\boldsymbol{J}\boldsymbol{M}^{-1}\boldsymbol{J}^T)^{-1} \\ \boldsymbol{\mu}(\boldsymbol{q},\dot{\boldsymbol{q}}) &= \bar{\boldsymbol{J}}^T\boldsymbol{b} - \boldsymbol{\Lambda}\dot{\boldsymbol{J}}\dot{\boldsymbol{q}} \\ \boldsymbol{p}(\boldsymbol{q}) &= \bar{\boldsymbol{J}}^T\boldsymbol{g} \\ \boldsymbol{\gamma} &= -\bar{\boldsymbol{J}}^T\boldsymbol{\Phi}^T(\boldsymbol{\alpha}+\boldsymbol{\rho}) \\ \bar{\boldsymbol{J}}^T &= \boldsymbol{\Lambda}\boldsymbol{J}\boldsymbol{M}^{-1} \end{aligned} \tag{68}$$

In applying (67) it is important to note that actuation may not exist at all of the physical joints described by the generalized coordinates. This is particulary true in the case of constrained systems such as parallel mechanisms where many of the joints are passive. We can resolve this fact in our control by using a selection matrix. Given a selection matrix for the actuated joints, $\boldsymbol{S} \in \mathbb{R}^{k\times n}$, we can express (67) as,

$$\bar{\boldsymbol{J}}^T\boldsymbol{\Theta}^T\boldsymbol{S}^T\boldsymbol{\tau}_k = \boldsymbol{\Lambda}\ddot{\mathbf{x}} + \boldsymbol{\mu} + \boldsymbol{p} + \boldsymbol{\gamma} \tag{69}$$

where $\boldsymbol{\tau} = \boldsymbol{S}^T\boldsymbol{\tau}_k$, and $\boldsymbol{\tau}_k$ is the $k \times 1$ vector of generalized forces acting at the k actuated joints. The matrix $\bar{\boldsymbol{J}}^T\boldsymbol{\Theta}^T\boldsymbol{S}^T$ has dimensions of $m_T \times k$. Thus, $k \geq m_T$ is a necessary condition for the system to yield a solution of $\boldsymbol{\tau}_k$ for an arbitrary acceleration, $\ddot{\mathbf{x}}$.

In practice we can design task motion control using estimates of the operational space dynamic properties. This yields the following dynamic compensation equation,

$$\bar{\boldsymbol{J}}^T \boldsymbol{\Theta}^T \boldsymbol{S}^T \boldsymbol{\tau}_k = \widehat{\boldsymbol{\Lambda}} \boldsymbol{f}^\star + \widehat{\boldsymbol{\mu}} + \widehat{\boldsymbol{p}} + \widehat{\boldsymbol{\gamma}} \tag{70}$$

where $\boldsymbol{f}^\star$ is the input of the decoupled system and we use the notation $\widehat{}$ to represent estimates of various quantities. Any suitable control law can be chosen to serve as this input. In particular, we can choose a linear control law of the form,

$$\boldsymbol{f}^\star = \boldsymbol{K}_p(\mathbf{x}_d - \mathbf{x}) + \boldsymbol{K}_v(\dot{\mathbf{x}}_d - \dot{\mathbf{x}}) + \ddot{\mathbf{x}}_d \tag{71}$$

The procedure applied to (39) can also be applied to (14). In this case, however, the task space mapping is associated with the minimal set of generalized coordinates, $\boldsymbol{q}_C$. We begin by recalling (14),

$$\boldsymbol{\tau}_p = \boldsymbol{M}_p(\boldsymbol{q})\, \ddot{\boldsymbol{q}}_p + \boldsymbol{b}_p(\boldsymbol{q}, \dot{\boldsymbol{q}}_p) + \boldsymbol{g}_p(\boldsymbol{q}) \tag{72}$$

We can relate a set of task coordinates, $\mathbf{x}$, to the coordinates, $\boldsymbol{q}_p$, by,

$$\dot{\mathbf{x}} = \boldsymbol{J}\dot{\boldsymbol{q}} = \boldsymbol{J}_p\left(\boldsymbol{q}\right)\dot{\boldsymbol{q}}_p \tag{73}$$

where,

$$\boldsymbol{J}_p\left(\boldsymbol{q}\right) = \boldsymbol{J}\boldsymbol{C} \tag{74}$$

is the task Jacobian with respect to the minimal set of coordinates. We can map (72) into any appropriate task space via the dynamically consistent inverse of $\boldsymbol{J}_p$. This yields [25],

$$\boldsymbol{f} = \boldsymbol{\Lambda}(\boldsymbol{q})\, \ddot{\mathbf{x}} + \boldsymbol{\mu}(\boldsymbol{q}, \dot{\boldsymbol{q}}_p) + \boldsymbol{p}(\boldsymbol{q}) \tag{75}$$

where,

$$\begin{aligned} \boldsymbol{\Lambda}(\boldsymbol{q}) &= (\boldsymbol{J}_p \boldsymbol{M}_p^{-1} \boldsymbol{J}_p^T)^{-1} \\ \boldsymbol{\mu}(\boldsymbol{q}, \dot{\boldsymbol{q}}_p) &= \bar{\boldsymbol{J}}_p^T \boldsymbol{b}_p - \boldsymbol{\Lambda} \dot{\boldsymbol{J}}_p \dot{\boldsymbol{q}}_p \\ \boldsymbol{p}(\boldsymbol{q}) &= \bar{\boldsymbol{J}}_p^T \boldsymbol{g}_p \\ \bar{\boldsymbol{J}}_p^T &= \boldsymbol{\Lambda} \boldsymbol{J}_p \boldsymbol{M}_p^{-1} \end{aligned} \tag{76}$$

We can express (75) in terms of the generalized forces,

$$\bar{\boldsymbol{J}}_p^T \boldsymbol{\tau}_p = \bar{\boldsymbol{J}}_p^T \boldsymbol{C}^T \boldsymbol{\tau} = \boldsymbol{\Lambda}\ddot{\mathbf{x}} + \boldsymbol{\mu} + \boldsymbol{p} \tag{77}$$

Given a selection matrix for the actuated joints, $\boldsymbol{S} \in \mathbb{R}^{k\times n}$, we can express (77) as,

$$\bar{\boldsymbol{J}}_p^T \boldsymbol{C}^T \boldsymbol{S}^T \boldsymbol{\tau}_k = \boldsymbol{\Lambda}\ddot{\mathbf{x}} + \boldsymbol{\mu} + \boldsymbol{p} \tag{78}$$

where $\boldsymbol{\tau}_p = \boldsymbol{C}^T\boldsymbol{\tau} = \boldsymbol{C}^T\boldsymbol{S}^T\boldsymbol{\tau}_k$. The matrix $\bar{\boldsymbol{J}}_p^T \boldsymbol{C}^T \boldsymbol{S}^T$ has dimensions of $m_T \times k$. Again, $k \geq m_T$ is a necessary condition for the system to yield a solution of $\boldsymbol{\tau}_k$ for an arbitrary acceleration, $\ddot{\mathbf{x}}$.

Using estimates of the operational space dynamic properties we have the following dynamic compensation equation,

$$\bar{\boldsymbol{J}}_p^T \boldsymbol{C}^T \boldsymbol{S}^T \boldsymbol{\tau}_k = \widehat{\boldsymbol{\Lambda}} \boldsymbol{f}^\star + \widehat{\boldsymbol{\mu}} + \widehat{\boldsymbol{p}} \tag{79}$$

where $\boldsymbol{f}^\star$ can be given by (71).

5.2 Task/Constraint Partitioning of Dynamics

In this formulation the multiplier form of the constrained equation of motion (7) is mapped into operational space using the dynamically consistent inverse of a Jacobian which characterizes both task and constraints [7]. The resulting operational space equation is then partitioned into an equation corresponding to task motion control, and an equation corresponding to constraint forces.

We begin by recalling the multiplier form of the constrained equation of motion (7),

$$\boldsymbol{\tau} + \boldsymbol{\Phi}^T \boldsymbol{\lambda} = \boldsymbol{M}\ddot{\boldsymbol{q}} + \boldsymbol{b} + \boldsymbol{g} \tag{80}$$

Again, we can relate a set of task coordinates, $\boldsymbol{x}$, to the set of generalized coordinates, $\boldsymbol{q}$, by,

$$\dot{\mathbf{x}} = \boldsymbol{J}\,\dot{\boldsymbol{q}} \tag{81}$$

in addition to the constraint condition,

$$\dot{\boldsymbol{\phi}} = \boldsymbol{\Phi}\dot{\boldsymbol{q}} = \mathbf{0} \tag{82}$$

We can concatenate (81) and (82) into a single vector,

$$\dot{\check{\mathbf{x}}} = \begin{pmatrix} \dot{\boldsymbol{x}} \\ \dot{\boldsymbol{\phi}} \end{pmatrix} = \begin{pmatrix} \boldsymbol{J} \\ \boldsymbol{\Phi} \end{pmatrix} \dot{\boldsymbol{q}} = \check{\boldsymbol{J}}\dot{\boldsymbol{q}} \tag{83}$$

where we use the notation ˇ to represent a quantity that is formed from the composition of task and constraint terms.

The active generalized force can be decomposed into a task space component and a null space component as in (47),

$$\boldsymbol{\tau} = \check{\boldsymbol{J}}^T \check{\boldsymbol{f}} + \check{\boldsymbol{N}}^T \boldsymbol{\tau}_o = \begin{pmatrix} \boldsymbol{J}^T & \boldsymbol{\Phi}^T \end{pmatrix} \begin{pmatrix} \boldsymbol{f} \\ \boldsymbol{f}_C \end{pmatrix} + \check{\boldsymbol{N}}^T \boldsymbol{\tau}_o \tag{84}$$

where $\boldsymbol{f}_C$ is the component of the applied operational space force acting along the constraint direction. Equation (80) can thus be written as,

$$\check{\boldsymbol{J}}^T \begin{pmatrix} \boldsymbol{f} \\ \boldsymbol{f}_C \end{pmatrix} + \check{\boldsymbol{N}}^T \boldsymbol{\tau}_o + \check{\boldsymbol{J}}^T \begin{pmatrix} \mathbf{0} \\ \boldsymbol{\lambda} \end{pmatrix} = \boldsymbol{M}\ddot{\boldsymbol{q}} + \boldsymbol{b} + \boldsymbol{g} \tag{85}$$

We can now map (85) into operational space using the dynamically consistent inverse of $\check{\boldsymbol{J}}$. This yields,

$$\begin{pmatrix} \boldsymbol{f} \\ \boldsymbol{f}_C \end{pmatrix} + \begin{pmatrix} \mathbf{0} \\ \boldsymbol{\lambda} \end{pmatrix} = \check{\boldsymbol{\Lambda}}(\boldsymbol{q}) \begin{pmatrix} \ddot{\mathbf{x}} \\ \mathbf{0} \end{pmatrix} + \check{\boldsymbol{\mu}}(\boldsymbol{q}, \dot{\boldsymbol{q}}) + \check{\boldsymbol{p}}(\boldsymbol{q}) \tag{86}$$

where the constraint condition, $\ddot{\boldsymbol{\phi}} = \mathbf{0}$, has been imposed. We have the following definitions,

$$\begin{aligned} \check{\boldsymbol{\Lambda}}(\boldsymbol{q}) &\triangleq \begin{pmatrix} \boldsymbol{J}\boldsymbol{M}^{-1}\boldsymbol{J}^T & \boldsymbol{J}\boldsymbol{M}^{-1}\boldsymbol{\Phi}^T \\ \boldsymbol{\Phi}\boldsymbol{M}^{-1}\boldsymbol{J}^T & \boldsymbol{\Phi}\boldsymbol{M}^{-1}\boldsymbol{\Phi}^T \end{pmatrix}^{-1} \\ \check{\boldsymbol{\mu}}(\boldsymbol{q}, \dot{\boldsymbol{q}}) &\triangleq \check{\boldsymbol{\Lambda}} \begin{pmatrix} \boldsymbol{J}\boldsymbol{M}^{-1}\boldsymbol{b} - \dot{\boldsymbol{J}}\dot{\boldsymbol{q}} \\ \boldsymbol{\Phi}\boldsymbol{M}^{-1}\boldsymbol{b} - \dot{\boldsymbol{\Phi}}\dot{\boldsymbol{q}} \end{pmatrix} \\ \check{\boldsymbol{p}}(\boldsymbol{q}) &\triangleq \check{\boldsymbol{\Lambda}} \begin{pmatrix} \boldsymbol{J}\boldsymbol{M}^{-1}\boldsymbol{g} \\ \boldsymbol{\Phi}\boldsymbol{M}^{-1}\boldsymbol{g} \end{pmatrix} \end{aligned} \tag{87}$$

While (86) expresses the combined task-constraint dynamics of our system it is useful to partition the dynamics in the following manner,

$$
\begin{array}{c}
\begin{pmatrix} \boldsymbol{f} \\ \boldsymbol{f}_C \end{pmatrix} + \begin{pmatrix} \mathbf{0} \\ \boldsymbol{\lambda} \end{pmatrix} = \\
\begin{pmatrix} \check{\boldsymbol{\Lambda}}_{11} & \check{\boldsymbol{\Lambda}}_{12} \\ \check{\boldsymbol{\Lambda}}_{21} & \check{\boldsymbol{\Lambda}}_{22} \end{pmatrix} \begin{pmatrix} \ddot{\mathbf{x}} \\ \mathbf{0} \end{pmatrix} + \begin{pmatrix} \check{\boldsymbol{\mu}}_1 \\ \check{\boldsymbol{\mu}}_2 \end{pmatrix} + \begin{pmatrix} \check{\boldsymbol{p}}_1 \\ \check{\boldsymbol{p}}_2 \end{pmatrix}
\end{array}
\tag{88}
$$

From this partitioning we have an equation corresponding to task motion control,

$$
\boldsymbol{f} = \check{\boldsymbol{\Lambda}}_{11}\ddot{\mathbf{x}} + \check{\boldsymbol{\mu}}_1 + \check{\boldsymbol{p}}_1 \tag{89}
$$

and an equation corresponding to constraint forces,

$$
\boldsymbol{f}_C + \boldsymbol{\lambda} = \check{\boldsymbol{\Lambda}}_{21}\ddot{\mathbf{x}} + \check{\boldsymbol{\mu}}_2 + \check{\boldsymbol{p}}_2 \tag{90}
$$

The constraint force vector, $\boldsymbol{\lambda}$, will always arise so as to satisfy (90), as dictated by constraint consistency. The component of applied operational space force, $\boldsymbol{f}_C$, acting along the constraint direction has no impact on the motion control of the task. Its only effect is on the constraint forces (values of $\boldsymbol{\lambda}$) that arise. Thus, all choices for $\boldsymbol{f}_C$ result in equivalent motion control of the system [13]. However, specific choices can be made to optimize the control with regard to desired constraint forces or to account for certain joints being unactuated. As an example of the latter case we may impose the condition that certain joints are unactuated. The following condition expresses the absence of actuation at those joints,

$$
\tilde{\boldsymbol{S}}(\boldsymbol{J}^T\boldsymbol{f} + \boldsymbol{\Phi}^T\boldsymbol{f}_C) = \mathbf{0} \tag{91}
$$

where $\tilde{\boldsymbol{S}} \in \mathbb{R}^{(n-k)\times n}$ is a selection matrix for the unactuated joints. That is, $\tilde{\boldsymbol{S}}$ selects the unactuated joints from the overall generalized force vector. Equation (91) would thus complement (89) and (90).

Using estimates of the operational space dynamic properties we have the following dynamic compensation equation,

$$
\boldsymbol{f} = \widehat{\check{\boldsymbol{\Lambda}}}_{11}\boldsymbol{f}^\star + \widehat{\check{\boldsymbol{\mu}}}_1 + \widehat{\check{\boldsymbol{p}}}_1 \tag{92}
$$

where $\boldsymbol{f}^\star$ can be given by (71). The constraint force control term, $\boldsymbol{f}_C$, can be resolved by using,

$$
\boldsymbol{f}_C + \boldsymbol{\lambda} = \widehat{\check{\boldsymbol{\Lambda}}}_{21}\boldsymbol{f}^\star + \widehat{\check{\boldsymbol{\mu}}}_2 + \widehat{\check{\boldsymbol{p}}}_2 \tag{93}
$$

in the case that the control is chosen with regard to optimizing the resulting constraint forces, or, by using (91) in order to account for certain joints being unactuated. *Figure 7* depicts an operational space tracking controller for a constrained system based on this partitioning approach.

5.3 Conditions on Motion Control

Figure 8 illustrates the necessary conditions for fully controlling the multibody system with respect to the system degrees of freedom and the task coordinates. For the system to be *motion actuated* the number of actuators must equal or exceed the

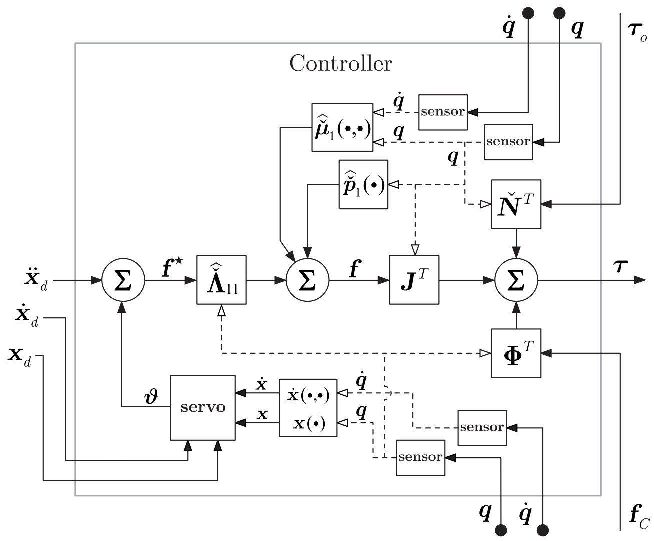

Figure 7: An operational space tracking controller for a constrained system. The desired task is tracked using appropriate dynamic compensation which accounts for the constraints. The terms $\boldsymbol{\tau}_o$ and $\boldsymbol{f}_C$ are chosen as part of the overall control design. An active applied torque is delivered to the plant.

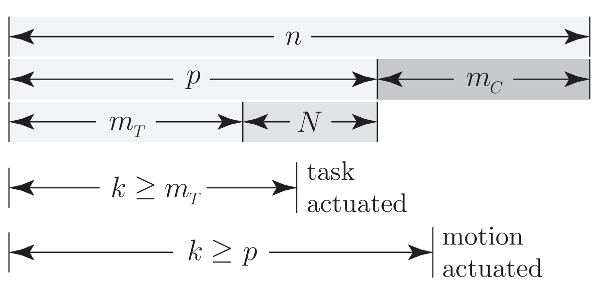

Figure 8: The relationship between the number of generalized coordinates - n, degrees of freedom - p, constraints - m_C, task coordinates - m_T, and null space coordinates - N. The system is *task actuated* if $k \geqslant m_T$ and *motion actuated* if $k \geqslant p$ where k is the number of actuators.

number of degrees of freedom, p. For the system to be *task actuated* the number of actuators must equal or exceed the number of task coordinates, m_T.

There are other conditions in addition to those stated above. Regarding task actuation, in the first formulation of *Section 5.1* the matrix $\bar{\boldsymbol{J}}^T \boldsymbol{\Theta}^T \boldsymbol{S}^T$ must be full rank. Similarly, in the second formulation of *Section 5.1* the matrix $\bar{\boldsymbol{J}}_p^T \boldsymbol{C}^T \boldsymbol{S}^T$ must be full rank. Finally, in the formulation of *Section 5.2* the matrix $\tilde{\boldsymbol{S}}\boldsymbol{\Phi}^T$ must be full rank.

5.4 Examples

The following examples focus on task motion control of constrained systems using the control decomposition that has been presented in *Section 5.2*.

5.4.1 Redundant chain with internal constraints

A redundant serial chain mechanism is depicted in *Figure 9*. We will impose constraints between the first three joints. These can be thought of as either servo constraints, if they are enforced by the controller, or constraints associated with the structure of the mechanism itself. The later case could, for example, correspond to a geared transmission (not shown in the figure) in which the second and third joints are coupled to the first joint. As an example of this we could specify the following set of constraint equations,

$$\boldsymbol{\phi}(\boldsymbol{q}) = \begin{pmatrix} q_2 - \frac{1}{3}q_1 \\ q_3 - \frac{2}{3}q_1 \end{pmatrix} \tag{94}$$

We now define a task to control the terminal point of the chain; that is, $\boldsymbol{x} \triangleq \boldsymbol{r}_E$. This represents an actual rheonomic servo constraint since it will be enforced by the controller. In this case the component of applied operational space force, $\boldsymbol{f}_C$, acting along the constraint direction will be chosen to be zero. If we interpreted the constraints in (94) to be servo constraints they would be incorporated into $\boldsymbol{x}$ rather then $\boldsymbol{\phi}$. This would change the control torques since the constraints would be enforced by the controller rather than the internal structure of the mechanism.

The 2-dimensional null space is controlled to minimize the gravity effort, defined as $U \triangleq \|\boldsymbol{g}(\boldsymbol{q})\|^2$. Our control torque is then,

$$\boldsymbol{\tau} = \boldsymbol{J}^T \boldsymbol{f} - K_N \check{\boldsymbol{N}}^T \frac{\partial U}{\partial \boldsymbol{q}} \tag{95}$$

where $\boldsymbol{f}$ is given by (92) and K_N is a null space gain. All joints are assumed to be actuated so no selection matrix needs to be introduced. Simulation plots for the system under a goal position command are shown in *Figures 9* and *10*. A linear (PD) control law is used as the input of the decoupled system (71). A small amount of damping was applied in the null space to damp out oscillations. In *Figure 10* we note that the gravity effort is minimized in a manner consistent with the task and constraints. We also see that the time histories of the first three joint torques exhibit some spikes due to the rapid and drastic changes in configuration induced by the gravity effort minimization.

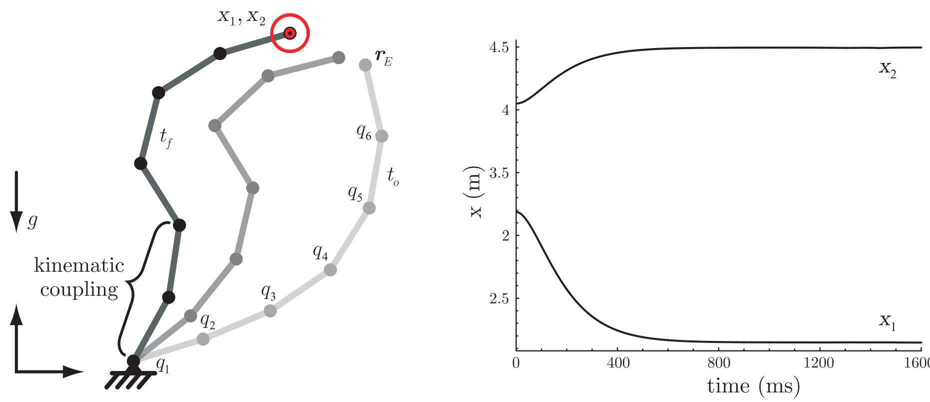

Figure 9: (Left) Redundant chain with internal joint constraints. The constraints kinematically couple the first three joints. The terminal point of the chain is being controlled. In this case $n = 6$, $m_T = 2$, and $m_C = 2$. (Right) Time response of the task coordinates. The control gains are $K_p = 100$, $K_v = 20$, and $K_N = 0.1$.

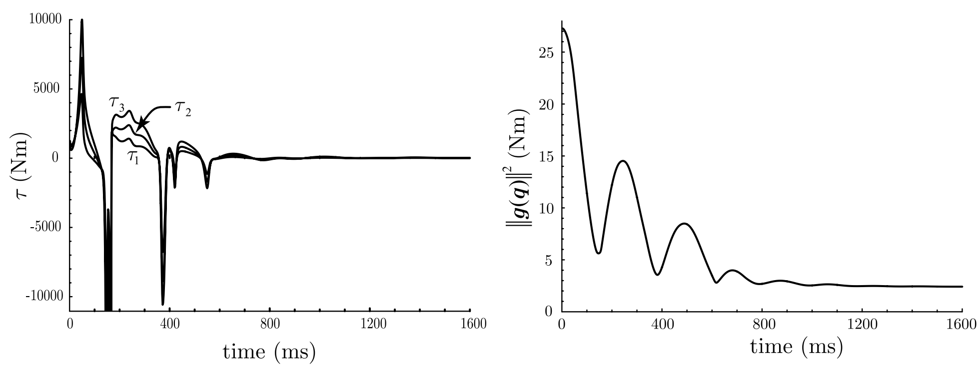

Figure 10: (Left) Time response of first three joints for the constrained redundant chain. Constraints are enforced consistent with (94). (Right) The 2-dimensional null space is being controlled to minimize gravity effort, $U = \|\boldsymbol{g}(\boldsymbol{q})\|^2$. The null space term, $-K_N \check{\boldsymbol{N}}^T \nabla U$, executes a task and constraint consistent minimization.

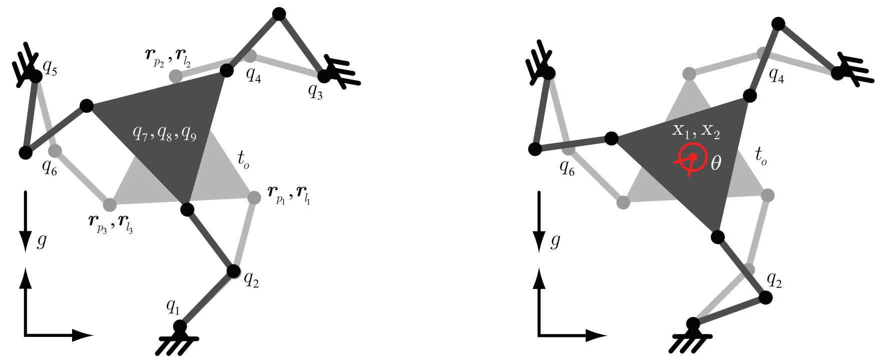

Figure 11: (Left) Parallel mechanism consisting of serial chains with loop closures. The three elbow joints are actively controlled while the remaining joints are passive. (Right) The orientation of the platform is commanded to rotate while its center is to remain fixed. In this case $n = 9$, $m_T = 3$, $m_C = 6$, and $k = 3$.

5.4.2 Mechanism with loop closures

A parallel mechanism is depicted in *Figure 11*. The constraint equations describe the loop closures and are given by,

$$\boldsymbol{\phi}(\boldsymbol{q}) = \begin{pmatrix} \boldsymbol{r}_{p_1} - \boldsymbol{r}_{l_1} \\ \boldsymbol{r}_{p_2} - \boldsymbol{r}_{l_2} \\ \boldsymbol{r}_{p_3} - \boldsymbol{r}_{l_3} \end{pmatrix} \tag{96}$$

The task is defined to control the active elbow joints; that is, $\mathbf{x} \triangleq \begin{pmatrix} q_2 & q_4 & q_6 \end{pmatrix}^T$. This corresponds to,

$$\boldsymbol{J} = \begin{pmatrix} 0 & 1 & 0 & 0 & 0 & 0 & 0 & 0 & 0 \\ 0 & 0 & 0 & 1 & 0 & 0 & 0 & 0 & 0 \\ 0 & 0 & 0 & 0 & 0 & 1 & 0 & 0 & 0 \end{pmatrix} \tag{97}$$

Due to the passive nature of all other joints the component of active force, $\boldsymbol{f}_C$, acting along the constraint direction is chosen to be zero. This can be derived from the condition of (91), where,

$$\tilde{\boldsymbol{S}} = \begin{pmatrix} 1 & 0 & 0 & 0 & 0 & 0 & 0 & 0 & 0 \\ 0 & 0 & 1 & 0 & 0 & 0 & 0 & 0 & 0 \\ 0 & 0 & 0 & 0 & 1 & 0 & 0 & 0 & 0 \\ 0 & 0 & 0 & 0 & 0 & 0 & 1 & 0 & 0 \\ 0 & 0 & 0 & 0 & 0 & 0 & 0 & 1 & 0 \\ 0 & 0 & 0 & 0 & 0 & 0 & 0 & 0 & 1 \end{pmatrix} \tag{98}$$

Since $\tilde{\boldsymbol{S}}\boldsymbol{J}^T\boldsymbol{f} = \boldsymbol{0}$,

$$\boldsymbol{f}_C = -(\tilde{\boldsymbol{S}}\boldsymbol{\Phi}^T)^{-1}\tilde{\boldsymbol{S}}\boldsymbol{J}^T\boldsymbol{f} = \boldsymbol{0} \tag{99}$$

There is no null space in this particular example so our control torque is given by $\boldsymbol{\tau} = \boldsymbol{J}^T\boldsymbol{f}$, where $\boldsymbol{f}$ is given by (92). *Figure 12* shows simulation plots for the

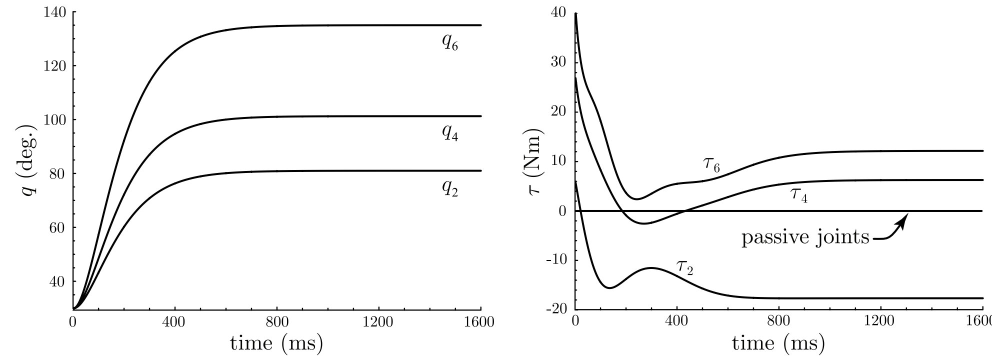

Figure 12: (Left) Time response of the elbow joints moving to a goal. (Right) Time response of the control torques during goal movement. Zero control torque is produced at the passive joints. The control gains are $K_p = 100$ and $K_v = 20$.

system under a goal position command. A linear (PD) control law is used as the input of the decoupled system.

In a second case we will define the task to control the position and orientation of the platform (see *Figure 11*); that is, $\mathbf{x} \triangleq (\ q_7 \quad q_8 \quad q_9\ )^T$. In this case $\boldsymbol{f}_C \neq \mathbf{0}$ since $\tilde{\boldsymbol{S}}\boldsymbol{J}^T\boldsymbol{f} \neq \mathbf{0}$. The orientation is commanded to rotate while the center of the platform is commanded to remain fixed. A linear (PD) control law is used as the input of the decoupled system. *Figure 13* shows simulation plots for the system under a goal position command.

5.4.3 Underactuated redundant chain

A redundant serial chain with an unactuated joint is depicted in *Figure 14*. The task is defined to control the terminal point of the chain, that is $\boldsymbol{x} \triangleq \boldsymbol{r}_E$. Since the number of actuators, $k = 2$, is less the number of degrees of freedom, $p = 3$, the system is under-actuated with respect to configuration space but sufficiently actuated with respect to the task dimension, $m_T = 2$. With joint 1 unactuated we have,

$$\tilde{\boldsymbol{S}} = \begin{pmatrix} 1 & 0 & 0 \end{pmatrix} \tag{100}$$

Simulation plots for the system under a goal position command are shown in *Figure 14* and *Figure 15*. A linear (PD) control law is used as the input of the decoupled system. The time response of the joint angles shows undamped null space oscillation due to the unactuated joint.

6 Inclusion of Flexible Bodies

The previous sections have detailed the control of constrained multibody systems where the bodies are rigid. These methods can be extended to handle constrained systems involving a mix of flexible and rigid bodies. The method of absolute nodal coordinates described by Shabana [26] has a demonstrated efficacy in application to flexible/rigid multibody systems. Using this method the flexible subsystems

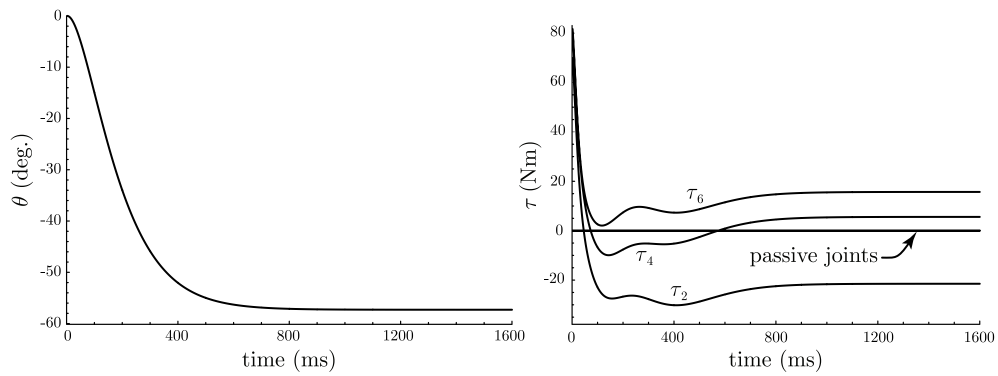

Figure 13: The orientation of the platform is commanded to rotate while its center is to remain fixed. (Left) Time response of the platform orientation. (Right) Time response of the control torques during goal movement. Zero control torque is produced at the passive joints. The control gains are $K_p = 100$ and $K_v = 20$.

are described using finite element nodal coordinates with respect to an absolute global coordinate system. For the rigid body subsystems we can choose generalized coordinates that describe relative joint motion. Coupling the flexible and rigid subsystems together results in a constrained dynamical system with graph topology.

The approaches presented in the previous sections offer a natural means of addressing the control of such systems. In this case the generalized coordinates consist of passive coordinates (finite element nodes) and active coordinates (actuated joints). The objective is to control certain rigid body coordinates as well as certain flexible body coordinates in order to achieve an overall task objective (see *Figure 16*). It is noted that there may be certain limitations regarding the degree to which the flexible coordinates can be controlled. This will be discussed in *Section 6.3*.

6.1 Flexible Body Dynamics

Kübler et al. [17] [18] provide an excellent description of the absolute nodal coordinate method with regard to flexible/rigid multibody systems. A brief review is presented here.

For a given flexible body subsystem a Lagrangian or material description is chosen which relates all quantities to the reference configuration, $\boldsymbol{X}$, of the system with domain Ω_o. Using a nonlinear finite element approach a set of shape or interpolating functions, $\{N_1, \cdots, N_s\}$, associated with a particular finite element discretization of s nodes can be chosen.

In the case of 8 node isoparametric hexahedral elements (see *Figure 17*) the interpolating functions are given as [12],

$$N_a(\boldsymbol{\xi}) = \frac{1}{8}(1+\xi_a\xi)(1+\eta_a\eta)(1+\zeta_a\zeta) \quad \text{for } a = 1, 2, \cdots, 8 \tag{101}$$

where $\boldsymbol{\xi} = \begin{pmatrix} \xi & \eta & \zeta \end{pmatrix}^T$ are the coordinates of the intrinsic element parameter space. For the higher order 27 node hexahedral element, Lagrange polynomials can

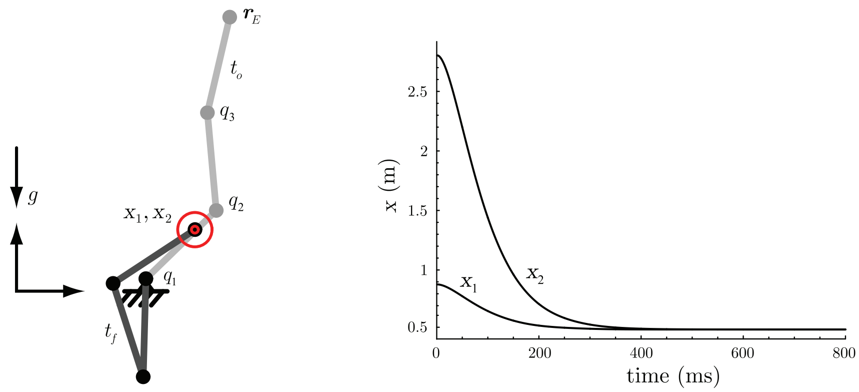

Figure 14: (Left) Under-actuated redundant chain. Joint 1 is unactuated (passive). In this case $n = 3$, $k = 2$, and $m_T = 2$. (Right) Time response of the task coordinates for the under-actuated system moving to a goal location. The control gains are $K_p = 100$ and $K_v = 20$.

be used to construct the interpolating functions [12]. Defining the shape matrix, $\boldsymbol{N} \in \mathbb{R}^{3\times 3s}$,

$$\boldsymbol{N} \triangleq \begin{pmatrix} N_1 & 0 & 0 & \cdots & N_s & 0 & 0 \\ 0 & N_1 & 0 & \cdots & 0 & N_s & 0 \\ 0 & 0 & N_1 & \cdots & 0 & 0 & N_s \end{pmatrix} \tag{102}$$

the displacement field, $\boldsymbol{u}(\boldsymbol{X}, t) \in \mathbb{R}^3$, is given by $\boldsymbol{u} = \boldsymbol{N}\boldsymbol{d}$, where $\boldsymbol{d} \in \mathbb{R}^{3s}$ is the vector of nodal displacements. The current material configuration is then given by $\boldsymbol{x}(\boldsymbol{X}, t) = \boldsymbol{X} + \boldsymbol{u}(\boldsymbol{X}, t)$. The weak form statement (summation convention applied) of the elastodynamics problem is,

$$\delta d_j (M_{jk}\ddot{d}_k + k_j + g_j) = 0 \tag{103}$$

where,

$$\begin{aligned} M_{jk} &= \int_{\Omega_o} \rho_o N_{ij} N_{ik} dV \\ k_j &= \int_{\Omega_o} \frac{\partial N_{ij}}{\partial X_k}(\delta_{il} + \frac{\partial N_{il}}{\partial X_k} d_k) S_{lk} dV \\ g_j &= -\int_{\Omega_o} \rho_o N_{ij} b_i dV - \int_{\partial\Omega_o} N_{ij} p_i dA \end{aligned} \tag{104}$$

The term ρ_o is the material density field in the reference configuration, b_i are the body forces (eg. gravity), p_i are the surface forces, δ_{il} is the Kronecker delta, and S_{lk} is the second Piola-Kirchoff stress tensor. The system can thus be stated as,

$$\boldsymbol{M}\ddot{\boldsymbol{d}} + \boldsymbol{k} + \boldsymbol{g} = \boldsymbol{0} \tag{105}$$

or more generally as,

$$\boldsymbol{M}\ddot{\boldsymbol{d}} + \boldsymbol{k} + \boldsymbol{g} = \boldsymbol{f} \tag{106}$$

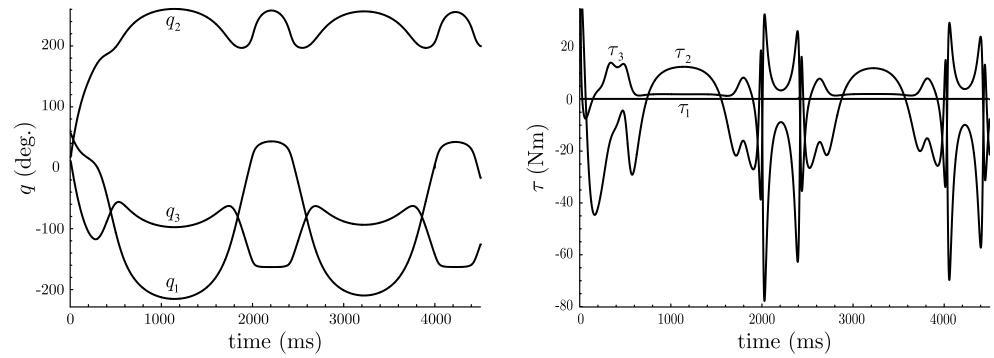

Figure 15: (Left) Time response of the joint angles for the under-actuated redundant chain showing undamped null space oscillation due to the unactuated joint. (Right) Time response of the control torques during goal movement. Zero control torque is produced at the passive joints. The control gains are $K_p = 100$ and $K_v = 20$.

where $\boldsymbol{f} \in \mathbb{R}^{3s}$ is a vector of external control forces applied at the nodes. The terms $\boldsymbol{M} \in \mathbb{R}^{3s\times 3s}$, $\boldsymbol{k} \in \mathbb{R}^{3s}$, and $\boldsymbol{g} \in \mathbb{R}^{3s}$ are the mass matrix, stiffness vector, and body/surface force vector respectively. It is noted that due to integration with respect to the reference configuration, Ω_o, the mass matrix, $\boldsymbol{M}$, is constant. The stress tensor, $\boldsymbol{S}$, is highly nonlinear however.

Different constitutive models can be applied yielding alternate weak form statements. In particular, viscous effects are important for some systems. Structural damping models are discussed in [18], however we will not consider these detailed constitutive models since it is assumed that the basic mathematical structure of (106) can still be achieved with these models. For the remainder of this section we will focus on the mathematical structure of (106) rather than the constitutive specifics of the terms.

6.2 Subsystem Assembly

We can assemble a set of rigid and flexible subsystems into single constrained system. First, we specify the dynamics of a set of y unconstrained rigid body subsystems,

$$\begin{aligned} \boldsymbol{\tau}_1 &= \boldsymbol{M}_{r_1}\ddot{\boldsymbol{q}}_1 + \boldsymbol{b}_1 + \boldsymbol{g}_{r_1} \\ &\vdots \\ \boldsymbol{\tau}_y &= \boldsymbol{M}_{r_y}\ddot{\boldsymbol{q}}_y + \boldsymbol{b}_y + \boldsymbol{g}_{r_y} \end{aligned} \tag{107}$$

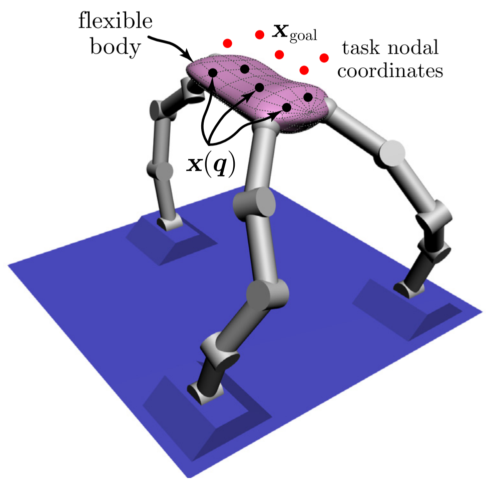

Figure 16: A rigid/flexible multibody system with constraints between the bodies. A set of nodal displacements are assigned as the task coordinates.

Next, we specify the dynamics of a set of z flexible subsystems which have been discretized using absolute nodal coordinates,

$$\begin{aligned} \boldsymbol{f}_1 &= \boldsymbol{M}_{f_1}\ddot{\boldsymbol{d}}_1 + \boldsymbol{k}_1 + \boldsymbol{g}_{f_1} \\ &\vdots \\ \boldsymbol{f}_z &= \boldsymbol{M}_{f_z}\ddot{\boldsymbol{d}}_z + \boldsymbol{k}_z + \boldsymbol{g}_{f_z} \end{aligned} \tag{108}$$

The sets of equations given by (107) and (108) can be assembled into a single system equation of the form,

$$\boldsymbol{\tau} = \boldsymbol{M}\ddot{\boldsymbol{q}} + \boldsymbol{b} + \boldsymbol{g} \tag{109}$$

where,

$$\begin{aligned} \boldsymbol{M} &= \operatorname{diag}(\boldsymbol{M}_{r_1}, \cdots, \boldsymbol{M}_{r_y}, \boldsymbol{M}_{f_1}, \cdots, \boldsymbol{M}_{f_z}) \\ \boldsymbol{\tau} &= \begin{pmatrix} \boldsymbol{\tau}_1^T & \cdots & \boldsymbol{\tau}_y^T & \boldsymbol{f}_1^T & \cdots & \boldsymbol{f}_z^T \end{pmatrix}^T \\ \ddot{\boldsymbol{q}} &= \begin{pmatrix} \ddot{\boldsymbol{q}}_1^T & \cdots & \ddot{\boldsymbol{q}}_y^T & \ddot{\boldsymbol{d}}_1^T & \cdots & \ddot{\boldsymbol{d}}_z^T \end{pmatrix}^T \\ \boldsymbol{b} &= \begin{pmatrix} \boldsymbol{b}_1^T & \cdots & \boldsymbol{b}_y^T & \boldsymbol{k}_1^T & \cdots & \boldsymbol{k}_z^T \end{pmatrix}^T \\ \boldsymbol{g} &= \begin{pmatrix} \boldsymbol{g}_{r_1}^T & \cdots & \boldsymbol{g}_{r_y}^T & \boldsymbol{g}_{f_1}^T & \cdots & \boldsymbol{g}_{f_z}^T \end{pmatrix}^T \end{aligned} \tag{110}$$

We have $\boldsymbol{M} \in \mathbb{R}^{n \times n}$ and $\boldsymbol{\tau}, \ddot{\boldsymbol{q}}, \boldsymbol{b}, \boldsymbol{g} \in \mathbb{R}^n$ where,

$$\begin{aligned} n &= \sum_{i=1}^{y} n_{r_i} + \sum_{i=1}^{z} n_{f_i} \\ n_{f_i} &= 3s_i \end{aligned} \tag{111}$$

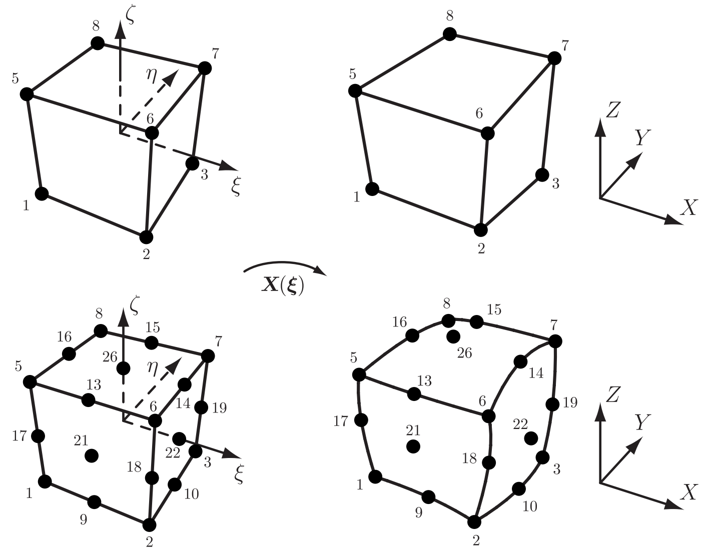

Figure 17: Isoparametric elements showing the mapping from the intrinsic parameter space, $\boldsymbol{\xi}$, to the physical space, $\boldsymbol{X}$. (Top) An 8 node hexahedral element (Bottom) A higher order 27 node hexahedral element.

Imposing a set of m_C holonomic constraint equations to establish system connectivity yields the familiar equation,

$$\boldsymbol{\tau} = \boldsymbol{M}\ddot{\boldsymbol{q}} + \boldsymbol{b} + \boldsymbol{g} - \boldsymbol{\Phi}^T \boldsymbol{\lambda} \tag{112}$$

subject to,

$$\boldsymbol{\Phi}\ddot{\boldsymbol{q}} + \dot{\boldsymbol{\Phi}}\dot{\boldsymbol{q}} = \boldsymbol{0} \tag{113}$$

6.3 Control Issues

We can apply the same control methodology to the constrained flexible/rigid multibody system described in *Section 6.2* that was applied to the constrained rigid multibody system addressed earlier in this paper. A number of issues need to be recognized however. Typically, flexible body subsystems will be passive. That is, there will be no control forces, $\boldsymbol{f}$, applied at the nodes. While a selection matrix, $\boldsymbol{S}$, can be used to specify the actuated coordinates, the rank conditions given in *Section 5.3* must still be satisfied (in addition to the condition on the number of actuators) to control the task nodal coordinates. Satisfying these rank conditions is problematic because the nodes in the flexible body subsystems are not kinematically coupled, as the bodies in the rigid body subsystems are, but rather *elastically* coupled. Sparseness of the mass matrices and task Jacobians of the flexible body subsystems is a consequence of this lack of kinematic coupling.

In rigid body systems, kinematic coupling allows a desired acceleration at the task control point to be achieved despite the lack of actuation at certain joints. This can be realized by recalling (69),

$$\bar{\boldsymbol{J}}^T \boldsymbol{\Theta}^T \boldsymbol{S}^T \boldsymbol{\tau}_k = \boldsymbol{\Lambda}\ddot{\mathbf{x}} + \boldsymbol{\mu} + \boldsymbol{p} + \boldsymbol{\gamma} \tag{114}$$

The matrix $\bar{\boldsymbol{J}}^T \boldsymbol{\Theta}^T \boldsymbol{S}^T$ must be full rank for there to be solution of actuator generalized forces to achieve an arbitrary task acceleration, $\ddot{\mathbf{x}}$. Kinematic coupling results in a dense task Jacobian and mass matrix, whereas elastic coupling in flexible systems results in a sparse task Jacobian and mass matrix. In this case, if the actuated nodal coordinates do not correspond to the nodal coordinates that constitute the task then the term $\bar{\boldsymbol{J}}^T \boldsymbol{\Theta}^T \boldsymbol{S}^T$ will be rank deficient. While this fact precludes finding a control input to achieve the desired task nodal accelerations at a given instant, control inputs may still exist that achieve the desired task nodal displacements in static equilibrium.

An additional consideration is that the task nodal displacements will typically be comprised of large rigid body displacements and small material deformations. As a practical matter if the specified desired nodal displacements involve large deformations the elastic forces will be large and the corresponding control input will be prohibitively large, particularly for stiff materials. Finally, it should be emphasized that applying this in an actual control system for a flexible/rigid multibody system requires sensing at the nodes of the flexible bodies.

7 Summary and Conclusions

In this paper we have presented a task-level methodology for the control of constrained multibody systems. This methodology exploits the natural symmetry between constrained dynamics and task space dynamics to synthesize dynamic compensation which properly accounts for the system constraints while performing a control task. The presence of passive joints in the constrained system has also been accommodated. A set of examples demonstrated the efficacy of this methodology in simulation. As a practical matter it is assumed that the controller has access to the system state (via a forward dynamics solver in the simulated case or via sensors in the physical case) and estimates of the dynamic properties of the physical system.

Application to flexible/rigid multibody systems was also addressed. The absolute nodal coordinate method can be used to describe the flexible bodies in conjunction with generalized coordinates that describe relative joint motion for the rigid bodies. A standard assembly procedure can be employed and connectivity constraints imposed to form a constrained flexible/rigid multibody system. The task-level control approaches presented here can then be applied in the same manner as with constrained rigid multibody systems. Since the nodes describing a flexible body are typically passive and elastically coupled there are limitations in controlling flexible body nodes as part of the task however. This is in contrast to passive joints between kinematically coupled rigid bodies.

The task-level constraint based control methods addressed here can be applied to motion control which involves contact with the environment. A particular application area for this is locomotion in robotic systems. The contact kinematics associated with intermittent foot/ground contact during gait can be modeled using constraints, as was done by Schiehlen [27]. The robot controller can thus employ a constraint based approach where transitions between different contact conditions can be detected and accommodated. This approach is applicable to a host of tasks outside of locomotion and represents a general methodology for constrained motion control.

Acknowledgments

The authors would like to thank Katherine Holzbaur for providing a motivation for this work with regard to constrained biomechanical systems. The helpful comments provided by Jaeheung Park and James Warren are also appreciated. Vincent De Sapio would like to thank Sandia National Laboratories for supporting this work.

References

[1] Bajodah, A. H., Hodges, D. H., and Chen, Y., "Inverse Dynamics of Servo-Constraints Based on the Generalized Inverse," *Nonlinear Dynamics*, vol. 39, pp. 179–196, 2005.

[2] Blajer, W., "A Geometric Unification of Constrained System Dynamics," *Multibody System Dynamics*, vol. 1, pp. 3–21, 1997.

[3] Blajer, W., and Kolodziejczyk, K., "A Geometric Approach to Solving Problems of Control Constraints: Theory and a DAE Framework," *Multibody System Dynamics*, vol. 11, pp. 343–364, 2004.

[4] Bruyninckx, H., and Khatib, O., "Gauss' Principle and the Dynamics of Redundant and Constrained Manipulators," In *Proceedings of the 2000 IEEE International Conference on Robotics and Automation*, vol. 3, pp. 2563–2568, San Francisco, April 2000.

[5] Craig, J. J., *Introduction to Robotics: Mechanics and Control*, 3rd ed., Upper Saddle River NJ: Prentice Hall, 2004.

[6] De Sapio, V., "Some Approaches for Modeling and Analysis of a Parallel Mechanism with Stewart Platform Architecture," In *Proceedings of the 1998 ASME International Mechanical Engineering Congress and Exposition*, MED-vol. 8, pp. 637–649, Anaheim CA, November 7, 1998.

[7] De Sapio, V., and Khatib, O., "Operational Space Control of Multibody Systems with Explicit Holonomic Constraints," In *Proceedings of the 2005 IEEE International Conference on Robotics and Automation*, vol. 1, pp. 470–475, Barcelona, April 2005.

[8] Delp, S. L., Loan, J. P., Hoy, M. G., Zajac, F. E., Topp, E. L., and Rosen, J. M., "An interactive graphics-based model of the lower extremity to study orthopaedic surgical procedures," *IEEE Transactions on Biomedical Engineering*, vol. 37, pp. 757–767, 1990.

[9] Gauss, K. F., "Über ein neues allgemeines Grundgesetz der Mechanik (On a New Fundamental Law of Mechanics)," *Journal für die Reine und Angewandte Mathematik*, vol. 4, pp. 232–235, 1829.

[10] Gibbs, J. W., "On the Funfamental Formulae of Dynamics," *American Journal of Mathematics*, vol. 2, pp. 49–64, 1879.

[11] Holzbaur, K. R. S., Murray, W. M., Delp, S. L., "A Model of the Upper Extremity for Simulating Musculoskeletal Surgery and Analyzing Neuromuscular Control," *Annals of Biomedical Engineering*, vol. 33, no. 6, pp. 829–840, 2005.

[12] Hughes, T.J.R., *The Finite Element Method: Linear Static and Dynamic Finite Element Analysis*, reprint, New York: Dover, 2000.

[13] Huston, R. L., Liu, C. Q., and Li, F., "Equivalent Control of Constrained Multibody Systems," *Multibody System Dynamics*, vol. 10, no. 3, pp. 313–321, October, 2003.

[14] Jungnickel, U., "Differential-Algebraic Equations in Riemannian Spaces and Applications to Multibody System Dynamics," *ZAMM*, vol. 74, no. 9, pp. 409–415, 1994.

[15] Khatib, O., "A Unified Approach to Motion and Force Control of Robot Manipulators: The Operational Space Formulation," *International Journal of Robotics Research*, vol. 3, no. 1, pp. 43–53, 1987.

[16] Khatib, O., "Inertial Properties in Robotic Manipulation: An Object Level Framework," *International Journal of Robotics Research*, vol. 14, no. 1, pp. 19–36, February, 1995.

[17] Kübler, L., Eberhard, P., and Geisler, J., "Flexible Multibody Systems with Large Deformations using Absolute Nodal Coordinates for Isoparametric Solid Brick Elements," In *Proceedings of the 2003 ASME Design Engineering Technical Conference*, September 2003.

[18] Kübler, L., Eberhard, P., and Geisler, J., "Flexible Multibody Systems with Large Deformations and Nonlinear Structural Damping Using Absolute Nodal Coordinates," *Nonlinear Dynamics*, vol. 34, no. 1–2, pp. 31–52, 2003.

[19] Lenarčič, J., and Stanišić, M. M., "A Humanoid Shoulder Complex and the Humeral Pointing Kinematics," *IEEE Transactions on Robotics and Automation*, vol. 19, no. 3, pp. 499–506, June 2003.

[20] Liu, Y.-H., Arimoto, S., Kitagaki, K., "Adaptive control for holonomically constrained robots: time-invariant and time-variant cases," In *Proceedings of the 1995 IEEE International Conference on Robotics and Automation*, vol. 1, pp. 905–912, Nagoya, Japan, May 1995.

[21] Liu, Y.-H., Kitagaki, K., Ogasawara, T., Arimoto, S., "Model-based adaptive hybrid control for manipulators under multiple geometric constraints ," *IEEE Transactions on Robotics and Automation*, vol. 7, no. 1, pp. 97–109, January 1999.

[22] Moon, F., *Applied Dynamics*, 1st ed., New York: John Wiley and Sons, 1998.

[23] Papastavridis, J.G., *Analytical Mechanics: A Comprehensive Treatise on the Dynamics of Constrained Systems for Engineers, Physicists, and Mathematicians*, Oxford university Press, 2002

[24] Pars, L. A., *A Treatise on Analytical Dynamics*, reprint, Woodbridge CT: Ox Bow Press, 1979.

[25] Russakow, J., Khatib, O., and Rock, S. M., "Extended Operational Space Formulation for Serial-to-Parallel Chain (Branching) Manipulators," In *Proceedings of the the 1995 IEEE International Conference on Robotics and Automation*, vol. 1, pp. 1056–1061, Nagoya, Japan, May 1995.

[26] Shabana, A., "Computer implementation of the absolute nodal coordinate formulation for flexible multibody dynamics," *Nonlinear Dynamics*, vol. 16, no. 3, pp. 293–306, July 1998.

[27] Schiehlen, W., "Energy-Optimal Design of Walking Machines," *Multibody System Dynamics*, vol. 13, no. 1, pp. 129–141, February, 2005.

[28] Udwadia, F. E., and Kalaba, R. E., *Analytical Dynamics: A New Approach*, 1st ed., Cambridge: Cambridge Uinversity Press, 1996.

[29] Wehage, R. A., and Haug, E. J., "Generalized Coordinate Partitioning for Dimension Reduction in Analysis of Constrained Dynamic Systems," *Journal of Mechanical Design*, vol. 104, no. 1, pp. 247–255, 1982.